CHEMMEDCHEM

DOI: 10.1002/cmdc.201000081

Discovery of Adamantyl Ethanone Derivatives as Potent 11β-Hydroxysteroid Dehydrogenase Type 1 (11β-HSD1) Inhibitors

Xiangdong Su,[a] Fabienne Pradaux-Caggiano,[a] Mark P. Thomas,[a] Michelle W. Y. Szeto,[a] Heather A. Halem,[b] Michael D. Culler,[b] Nigel Vicker,[a] and Barry V. L. Potter*[a]

11β-Hydroxysteroid dehydrogenases (11β-HSDs) are key enzymes regulating the pre-receptor metabolism of glucocorticoid hormones. The modulation of 11β-HSD type 1 activity with selective inhibitors has beneficial effects on various conditions including insulin resistance, dyslipidemia and obesity. Inhibition of tissue-specific glucocorticoid action by regulating 11β-HSD1 constitutes a promising treatment for metabolic and cardiovascular diseases. A series of novel adamantyl ethanone compounds was identified as potent inhibitors of human 11β-HSD1. The most active compounds identified (**52**, **62**, **72**, **92**, **103** and **104**) display potent inhibition of 11β-HSD1 with IC_{50} values in the 50–70 nM range. Compound **72** also proved to be metabolically stable when incubated with human liver microsomes. Furthermore, compound **72** showed very weak inhibitory activity for human cytochrome P450 enzymes and is therefore a candidate for in vivo studies. Comparison of the publicly available X-ray crystal structures of human 11β-HSD1 led to docking studies of the potent compounds, revealing how these molecules may interact with the enzyme and cofactor.

Introduction

Metabolic syndrome is a condition characterised by a cluster of disorders including insulin resistance, glucose intolerance, visceral obesity, hypertension and dyslipidemia, which are widely recognised as high risk factors for cardiovascular disease.[1] The rapidly increasing prevalence of metabolic syndrome has focused the need for novel treatments, thus attracting intense interest from pharmaceutical research laboratories across academia and industry. Glucocorticoid hormones play essential roles in the regulation of carbohydrate, lipid and bone metabolism, modulation of inflammatory responses, brain function and stress. Excessive glucocorticoid action is, in many aspects, associated with insulin and leptin resistance, leading to the development of obesity, type 2 diabetes and other metabolic and cardiovascular disorders, the major underlying causes of metabolic syndrome.[2–5] Numerous studies have implicated glucocorticoid action in the regulation of hepatic gluconeogenesis and lipogenesis, glucose uptake and lipid oxidation in skeletal muscle, and the production of angiotensinogen.[6–8] Patients with Cushing's syndrome have increased glucocorticoid exposure and exhibit similar symptoms compared with those with metabolic syndrome, including insulin resistance, high adiposity, dyslipidemia and hypertension.[9] These metabolic abnormities in Cushing's syndrome could be improved to a certain degree by decreasing the excessive glucocorticoid action through surgery or glucocorticoid receptor antagonist treatment.[10–12] The link between the similar phenotype of Cushing's syndrome and metabolic syndrome suggested the potential treatments of individual indications of metabolic syndrome by suppression of glucocorticoid activity.[13]

However, circulating glucocorticoid levels are not elevated in patients with the common form of obesity or overweight type 2 diabetes.[14] Therefore, it is speculated that intercellular levels of glucocorticoid, regulated by pre-receptor metabolism, are responsible for metabolic abnormalities. The pre-receptor metabolism of the active glucocorticoid cortisol (**2a**) and its precursor cortisone (**1a**) is mediated by 11β-hydroxysteroid dehydrogenase isozymes (11β-HSDs), which are microsomal enzymes from the short-chain dehydrogenase/reductase (SDR) superfamily.[15] Currently, two different 11β-HSD isozymes (11β-HSD1 and 11β-HSD2) have been reported in humans. The 11β-HSD1 isoform, highly expressed in liver and adipose tissue, converts cortisone (**1a**) in humans (11-dehydrocorticosterone **1b** in rodents) to the active glucocorticoid cortisol (**2a**) (corticosterone **2b** in rodents) in a NADPH dependent manner, thereby locally amplifying the glucocorticoid action in specific tissues (Scheme 1).[16,17] The 11β-HSD2 isoform is exclusively NAD^+ dependent and is mainly found in mineralocorticoid target tissues, such as the kidney and colon. The function of 11β-HSD2 is in inactivating physiological glucocorticoid cortisol to inactive cortisone in specific tissues, thereby preventing glucocorticoid occupation of the mineralocorticoid receptor (MR), which may lead to sodium retention, hypokalemia and hypertension.[18,19]

[a] *Dr. X. Su, Dr. F. Pradaux-Caggiano, Dr. M. P. Thomas, Dr. M. W. Y. Szeto, Dr. N. Vicker, Prof. B. V. L. Potter*
Medicinal Chemistry, Department of Pharmacy and Pharmacology and Sterix Ltd., University of Bath, Bath, BA2 7AY (UK)
Fax: (+44) 1225-386114
E-mail: B.V.L.Potter@bath.ac.uk

[b] *Dr. H. A. Halem, Dr. M. D. Culler*
IPSEN, Biomeasure Inc., 27 Maple Street, Milford, MA 01757 (USA)

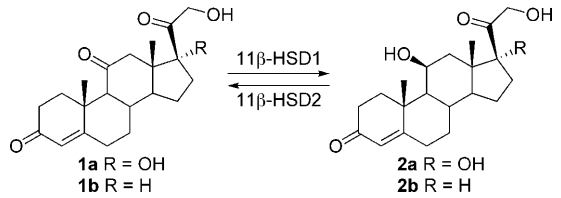

Scheme 1. Interconversion of glucocorticoid hormones catalysed by 11β-HSDs.

Studies revealed that 11β-HSD1 expression is increased in the adipose tissue of obese subjects suggesting the possibility of tissue-specific glucocorticoid excess.[20,21] Transgenic mice overexpressing 11β-HSD1 selectively in adipose tissue exhibited insulin-resistant diabetes, hyperlipidemia and visceral obesity.[22] Conversely, overexpression of 11β-HSD2 in transgenic mice resulted in greater insulin sensitivity, glucose tolerance and resistance to body weight gain on a high-fat diet.[23] In addition, the 11β-HSD1 knock-out mice are resistant to stress-induced hyperglycaemia and have decreased cholesterol and triglyceride levels.[24,25] It has also been shown that the modulation of 11β-HSD1 activity with selective inhibitors has beneficial effects on various conditions, including insulin resistance, dyslipidemia and obesity.[26–28] Furthermore, clinical studies showed that treatment with carbenoxolone, a nonselective inhibitor of 11β-HSDs, results in increased hepatic insulin sensitivity along with decreased glucose production.[29,30] More recently, positive proof-of-concept results from a 28 day phase IIa clinical trial with the 11β-HSD1 inhibitor INCB013739 (structure unknown) were reported by Incyte. In this trial, the treatment of type 2 diabetes mellitus patients with INCB013739 for 28 days significantly improved hepatic and peripheral insulin sensitivity and decreased fasting plasma glucose, low density lipoprotein and total cholesterol levels.[31] Inhibition of tissue-specific glucocorticoid action by regulating 11β-HSD1 constitutes a promising treatment for metabolic and cardiovascular diseases and therefore has attracted considerable attention over the last few years.[13,32–35] Increased research efforts by the pharmaceutical industry have led to the discovery of numerous types of potent, selective 11β-HSD1 inhibitors, and the progress in this area has been recently reviewed.[35–40] Compounds **3**–**7** are examples of potent 11β-HSD1 inhibitors on which advanced preclinical studies or clinical studies have been performed.[28,41–46]

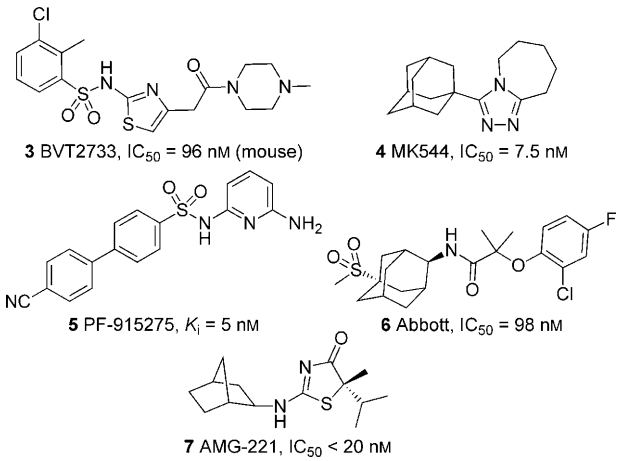

To discover novel, clinically useful inhibitors of 11β-HSD1, it is important to have an array of structural types of inhibitors, as the physicochemical properties of the compounds will determine tissue distribution, hypothalamic–pituitary–adrenal axis effects, and, ultimately, clinical utility. Therefore, we performed optimisation on hit compounds **8** and **9**, which we discovered previously, to improve potency.[47,48] We synthesised compounds containing an adamantyl group linked to an aromatic unit through a multi-atom linker with a carbonyl group attached to the adamantane as illustrated by general structure **10**. These target compounds were screened for their inhibitory activity against human 11β-HSD1 in a HEK293 cell-based assay. Herein, we report the discovery and the structure–activity relationships of some adamantyl ethanone compounds as potent inhibitors of 11β-HSD1.

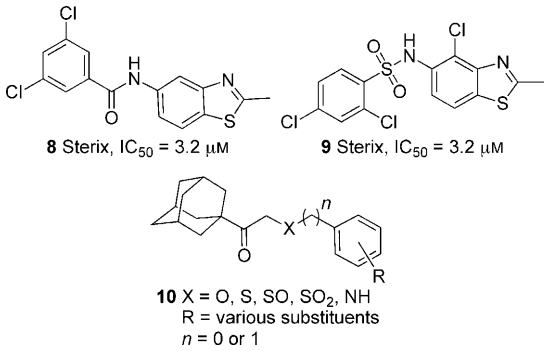

Results and Discussion

Chemistry

The target compounds **11**–**14** listed in Table 1, containing an amino ethanone linker, were synthesised by a nucleophilic coupling reaction between the aromatic amine and an aryl bromomethyl ketone or 1-adamantyl bromomethyl ketone in the presence of a base (Scheme 2).

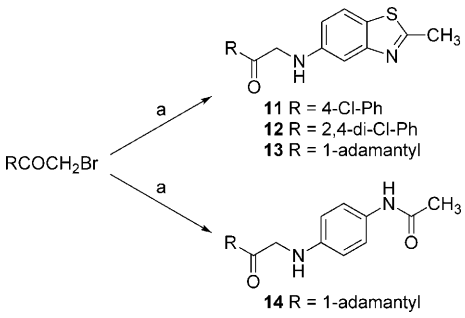

Scheme 2. Synthesis of the ethanone amine linker compounds **11**–**14**. *Reagents and conditions*: a) $ArNH_2$, K_2CO_3, CH_3CN or EtOH, RT, 12–24 h, 40–70%.

Similarly, target compounds **15**–**39**, with an ethanone ether linker, were generated by a nucleophilic coupling reaction between the corresponding phenols or benzyl alcohols and 1-adamantyl bromomethyl ketone under basic conditions in moderate to quantitative yields (Scheme 3).

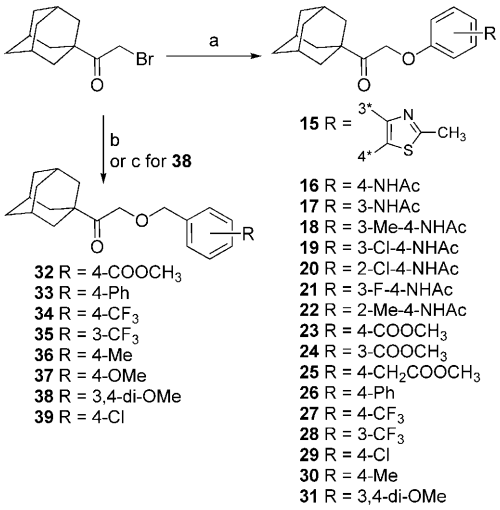

Scheme 3. Synthesis of ethanone ether linker compounds **15**–**39** (**3*** and **4*** indicate points of attachment to the phenyl ring). *Reagents and conditions*: a) ArOH, K_2CO_3, acetone or DMF, RT, 8–24 h, 37–100%; b) $ArCH_2OH$, NaH, THF, 0 °C; c) $ArCH_2OH$, *t*BuOK, toluene, RT, 16–36 h, 15–43%.

Target compounds **42**–**58**, with a carboxamide substituent on the phenyl ring, were generated in three steps by a nucleophilic substitution reaction of 1-adamantyl bromomethyl ketone with the corresponding methyl-ester-substituted phenols to form compounds **23** or **24**, then saponification of the esters to give **40** or **41**, followed by amide coupling of the required amine and phenyl acid (Scheme 4). Similarly, compounds **61**–**73**, with an acetamide substituent on the phenyl ring, were also prepared by the same method from **59** or **60** (obtained from the hydrolysis of **25** or **32**, respectively) as illustrated in Scheme 4.

The coupling reaction of 1-adamantyl bromomethyl ketone with the corresponding mercaptans in the presence of triethylamine in acetonitrile generated the target compounds **74**–**82**, which were then transformed into their corresponding sulfoxide **83**–**90** and sulfone analogues **91**–**99** by oxidation with *m*-CPBA at low temperature. Normally, the oxidation would produce both the sulfoxide (major) and the sulfone (minor); in some cases when only the sulfoxide was obtained, further oxidation with *m*-CPBA at room temperature was used to prepare the sulfone. Compounds **101**–**104** with a carboxamide substituent on the *meta* position of the phenyl ring were synthesised from **100** by an amide coupling to give **101** or **102** followed by oxidation of **102** to yield **103** and **104** (Scheme 5).

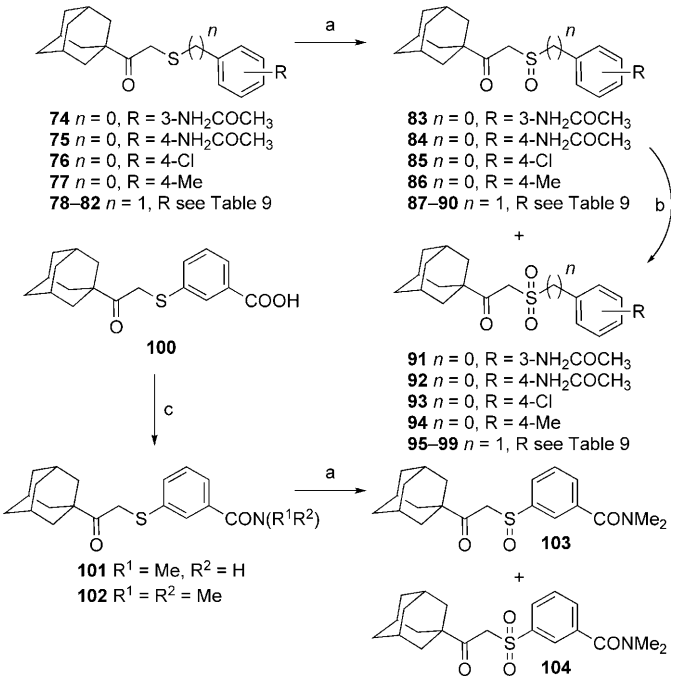

Scheme 5. Synthesis of ethanone sulfur linker compounds **74**–**104**. *Reagents and conditions*: a) *m*-CPBA, CH_2Cl_2, −10→0 °C, 20–90 min, 20–80%; b) *m*-CPBA, CH_2Cl_2, RT, 4–8 h, 29–94%; c) NHR^1R^2, EDCI, DMAP, Et_3N, CH_2Cl_2, RT, 16 h, 65–68%.

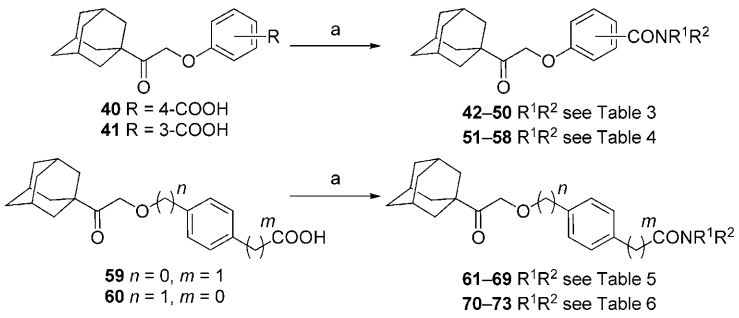

Scheme 4. Synthesis of ethanone ether linker compounds **40**–**73**. *Reagents and conditions*: a) NHR^1R^2, EDCI, DMAP, Et_3N, CH_2Cl_2, RT, 16–24 h, 25–88%.

Structure–activity relationships

The target compounds were examined for their inhibitory activity against 11β-HSD1 on HEK293 cell line. Because nontransfected HEK293 cells lack endogenous 11β-HSD1 activity, this cell line has been shown to be a suitable system for evaluating 11β-HSD1 activity after being transfected with the plasmid for expression of 11β-HSD1. The percent inhibition of 11β-HSD1 was measured at 1 μM in duplicate. The IC_{50} values are reported as the mean value of three measurements with variance of less than 20%.

Our earlier work identified a class of phenyl carboxamides and phenyl sulfonamides as inhibitors of human 11β-HSD1.[47,48] Compounds **8** and **9** exhibited moderate activity against purified human 11β-HSD1 with both having IC_{50} values of 3.2 μM, but had only very weak inhibition in the cell-based assay (< 50% inhibition at 10 μM).[47,48] The carboxamide group of compound **8** was then modified to break the conju-

gation in the linker. Compounds with an extended ethanone tethered to the methylbenzothiazole unit through an amino group were synthesised and screened for inhibition of 11β-HSD1. Compounds **11** and **12** showed improved activity on a transfected HEK293 cell line with IC_{50} values of 6.4 and 5.8 μM, respectively (Table 1).

Table 1. In vitro inhibition of compounds **11**–**15**.

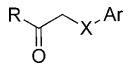

Compd	X	R	Ar[a]	IC_{50} [nM]
11	NH	4-Cl-Ph	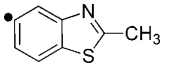	6400
12	NH	2,4-di-Cl-Ph	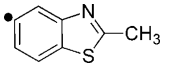	5800
13	NH	1-Adamantyl	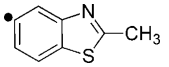	302
14	NH	1-Adamantyl	4-Acetamidophenyl	90
15	O	1-Adamantyl	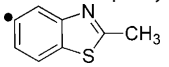	4755

[a] ●: Indicates point of attachment.

The adamantyl moiety has appeared in several potent 11β-HSD1 inhibitors.[28,43] The replacement of the chlorinated phenyl group with a more hydrophobic adamantyl moiety was a successful attempt to produce more potent compounds. The activity of compound **13** increased by ~20-fold with an IC_{50} value of 302 nM, which indicated that the adamantyl group was highly favoured with such a linker system possibly due to the hydrophobic interactions in the binding region. However, changing the amino group in the linker to oxygen was not well tolerated, and this modification lowered the inhibition to the same level as compound **15** with an IC_{50} value of 4.8 μM. The reason for this loss of activity could be a geometrical change in the linker affecting the position of the biaryl unit or the ability of the amino group in the linker to act as a hydrogen-bond donor giving added interactions with the protein backbone. The introduction of a 4-acetamidophenyl group, a more flexible aromatic motif than the benzothiazole group, gave compound **14** with ~3.5-fold improvement in activity and an IC_{50} value of 90 nM. The 4-acetamido moiety on the phenyl ring has both hydrogen-bond accepting and donating capabilities and may participate in a hydrogen bonding network with amino acid residues in the active site.

A series of compounds with phenyl rings substituted with hydrogen bonding groups, such as an acetamide, was then synthesised (Table 2). The ethanone amino linker was replaced with an ethanone ether linker to give compounds **16** and **17**; a loss of two- to threefold activity relative to **14** was observed, but the activity was retained with IC_{50} values of ~200–300 nM. These results suggest that an oxygen linker can indeed be tolerated in the case of a monocyclic aromatic ring, and that the acetamido substituent is acceptable at either the *para* or *meta* positions. Further modifications were performed by introducing a halogen or methyl substituent in the 2- or 3-positions on the 4-acetaminophenyl unit to give compounds **18**–**22**. With 3-fluoro or 2-methyl substituents, moderate inhibition of 11β-HSD1 was observed for compounds **21** and **22**, with IC_{50} values of ~900 nM, giving about a fourfold decrease in activity compared with **16**. These substitutions might be affecting the spatial position of the aryl ring or the acetamide group resulting in some loss of activity. Compounds **18**–**20** with methyl or chloro substituents showed only moderate inhibition when tested at 1 μM. The changes in the substituent in compounds **18**–**22** are not dramatic and so the loss of activity with these compounds compared with **16** indicates a lack of tolerance to substitution in this region. Surprisingly, when the ethanone ether linker was altered to a similar ethanone sulfide linker, the *meta*-acetamido compound (**74**) showed about a sevenfold loss of activity with an IC_{50} value of only ~2 μM. Nevertheless, the oxidation of the sulfide to the sulfoxide or sulfone raised the inhibitory activity into the 100 nM range (**83** and **91**), suggesting the oxygen or the sulfur atom possibly forms further interactions with the enzyme or alters the geometry of the molecule placing the adamantyl and/or the acetamidophenyl group in a position with improved binding in the active site. The same principle was applied to the *para*-acetamido series with similar encouraging results. Compounds **75**, **84** and **92** exhibited good activity with IC_{50} values of 313 nM, 151 nM and 58 nM, respectively. The activity of compound **75** is 6.5-fold more potent than **74**, a dramatic leap in activity for such a small change, probably indicating a subtle electronic effect in this region. The results for compounds **84** and **92** suggest that the ethanone sulfone or sulfoxide moieties can not only alter the geometry of the compound but are likely to enable additional hydrogen-bond interactions with the enzyme. The SO_2 group is found as part of linker system in known potent inhibitors.[41,42] Compound **92** with an IC_{50} value of 58 nM is the most active in this series and is indeed a potent novel inhibitor of human cellular 11β-HSD1.

Table 2. In vitro inhibitory activity of acetamido benzene derivatives.

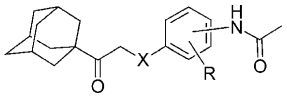

Compd	X	Acetamide	R	IC_{50} [nM]
16	O	*p*	–	211
17	O	*m*	–	285
18	O	*p*	3-Me	68%[a]
19	O	*p*	3-Cl	49%[a]
20	O	*p*	2-Cl	61%[a]
21	O	*p*	3-F	894
22	O	*p*	2-Me	897
74	S	*m*	–	2037
75	S	*p*	–	313
83	SO	*m*	–	105
84	SO	*p*	–	151
91	SO_2	*m*	–	167
92	SO_2	*p*	–	58

[a] Percent inhibition measured at a concentration of 1 μM.

Based on the positive results from the acetamido series, the possibility of altering the acetamido phenyl unit to a benzamide or phenylacetamide group was explored, as both of these moieties have hydrogen bonding capacity in the aromatic region. This would allow diverse substitution on the phenyl ring. Four structurally different subfamilies of compounds were made from readily available intermediates: *para*- or *meta*-benzamides with an ethanone linker (Tables 3 and 4), *para*-phenylacetamides with an ethanone linker (Table 5) and *para*-benzamides with an extra methylene unit in the linker (Table 6).

Table 3. In vitro inhibitory activity of 4-benzamide derivatives.

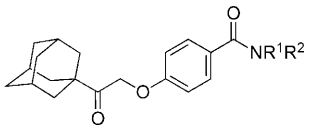

Compd	R^1	R^2	IC_{50} [nM]
42	H	H	117
43	H	Me	63 %[a]
44	H	Et	382
45	H	*i*Pr	594
46	H	*t*Bu	1140
47	Et	Et	798
48	H	Ph	283
49	H	Bn	1959
50	H	2-Furfuryl	69 %[a]

[a] Percent inhibition measured at a concentration of 1 μM.

Table 4. In vitro inhibitory activity of 3-benzamide derivatives.

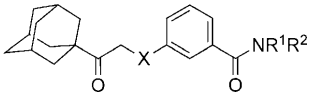

Compd	X	R^1	R^2	IC_{50} [nM]
51	O	H	H	1047
52	O	H	Me	68
53	O	H	Et	343
54	O	H	*i*Pr	1222
55	O	H	*t*Bu	59 %[a]
56	O	H	2-Furfuryl	229
57	O	H	Bn	527
58	O	H	Ph	876
101	S	H	Me	124
102	S	Me	Me	146
103	SO	Me	Me	57
104	SO_2	Me	Me	69

[a] Percent inhibition measured at a concentration of 1 μM.

Interestingly, we discovered that the nonsubstituted *para*-benzamide **42** had an IC_{50} value of 117 nM, while alkyl-substituted compounds like the methyl (**43**), ethyl (**44**), isopropyl (**45**) or *tert*-butyl (**46**) derivatives all showed lower activity, indicating that a bulky alkyl group in this region is not well tolerated (Table 3). This is also true for the *N*,*N*-diethylbenzamide compound (**47**) with an IC_{50} value of 798 nM. The *N*-phenylcarboxamide derivative (**48**) gave an interesting IC_{50} value of 283 nM, suggesting possibly a further aromatic interaction in that area. However, if another degree of rotation was given to the aromatic ring, as in the case of a benzyl-substituted compound (**49**), the activity decreased by sevenfold. A similar result was observed with a 2-furfuryl substituent (**50**).

Moving the carboxamide group from the *para* to the *meta* position led to some interesting findings. The nonsubstituted *meta*-benzamide **51** exhibited only moderate inhibitory activity with an IC_{50} value of 1 μM, a ninefold decrease relative to the *para* analogue **42**, whereas the 3-methylbenzamide **52** showed very good potency with an IC_{50} value of 68 nM. It is possible that the methyl group in the *meta* position is able to form hydrophobic interactions in the restricted space of the enzyme pocket, whereas a methyl group in the *para* position is not placed to pick up these additional interactions. The tendency to lose activity was observed for bulkier groups similar to the *para*-substituted series in Table 3, as moving from ethyl (**53**), to isopropyl (**54**) or *tert*-butyl (**55**) showed a decrease of activity. The 2-furfuryl analogue **56** was better tolerated than the benzyl **57** and phenyl **58** derivatives, with an IC_{50} value of 229 nM versus 527 and 876 nM, respectively. This observation is different to the *para*-carboxamide series suggesting that the aromatic interaction with the enzyme is restricted in certain areas. When the oxygen atom of the linker was substituted for a sulfur atom, the *N*-methyl- and *N*,*N*-dimethylbenzamide compounds **101** and **102** displayed similar potencies with IC_{50} values of 124 and 146 nM, respectively; a twofold loss of activity relative to the *N*-methylbenzamide **52** with the ethanone ether linker. However, with highly polarised linkers like the sulfoxide **103** or the sulfone **104** in the *N*,*N*-dimethylbenzamide series, compounds regained activity to give the most potent compounds in this series with IC_{50} values of ~60–70 nM, which indicates that a sulfone or sulfoxide unit of the linker is forming further interactions with the active site.

Replacement of the carboxamide with the acetamide group gives extra flexibility to the side chain. In the *para*-acetamide series, the IC_{50} value of the *N*-methyl substituted compound (**61**) was 94 nM (Table 5), much more potent than the *para*-carboxamide analogue **43** and similar to the *meta* analogue **52**, suggesting the extra flexibility may enable the methyl group to reach a binding region like the *meta* substituent. The extended acetamide compounds are able to interact with the enzyme in a fashion similar to the previously described carboxamide family. The potent activity of the *N*,*N*-dimethylacetamide **62** (IC_{50} = 58 nM) indicates that a hydrogen-bond donor attached to the phenyl ring is not required for activity, and the combination of the amide carbonyl acting as a hydrogen-bond acceptor and the *N*,*N*-dimethyl substituent being able to pick up added hydrophobic interactions improves potency. The nonsubstituted acetamide **63** showed a decreased activity with an IC_{50} value of 204 nM possibly due to some loss of hydrophobic binding with the enzyme. Bulky alkyl substituents are not well tolerated with the *N*-ethyl compound (**64**) losing activity by approximately fourfold and the isopropyl (**65**) and *tert*-butyl compounds (**66**) showing weaker inhibition as previously observed with enlarged steric bulk (compounds **44**–**46** in Table 3 and **53**–**55** in Table 4). Some aromatic interactions with

Table 5. In vitro inhibitory activity of 4-phenylacetamide derivatives.

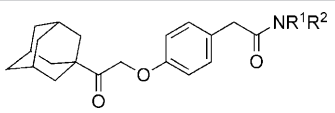

Compd	R^1	R^2	IC_{50} [nM]
61	H	Me	94
62	Me	Me	58
63	H	H	204
64	H	Et	912
65	H	*i*Pr	63 %[a]
66	H	*t*Bu	45 %[a]
67	H	Bn	472
68	H	Ph	2194
69	H	2-Furfuryl	4 %[a]

[a] Percent inhibition measured at a concentration of 1 μM.

the enzyme may be present as the benzyl derivative (**67**) had an IC_{50} value of 472 nM, whereas the phenyl (**68**) and 2-furfuryl compounds (**69**) lost activity indicating that the size and position of the aromatic group in the active site are important for activity.

The flexibility of the linker was also modified by adding an extra methylene group between the oxygen and the phenyl ring. A trend similar to that in the phenylacetamide series was observed (Table 6). The unsubstituted carboxamide **70** and the

Table 6. In vitro inhibitory activity of 4-benzamide derivatives.

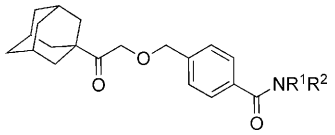

Compd	R^1	R^2	IC_{50} [nM]
70	H	H	63 %[a]
71	H	Me	250
72	Me	Me	56
73	H	Bn	69 %[a]

[a] Percent inhibition measured at a concentration of 1 μM.

N-benzyl compound **73** showed weaker activities, which might indicate that the lack of hydrophobic or aromatic interactions in this region has negative effects on the inhibitory activity. On the other hand the activity of the *N*-methyl compound (**71**), with an IC_{50} value of 250 nM, indicates that hydrophobic interactions limited to a confined region are preferred. Furthermore, the combination of the extended ethanone linker and phenyl *N*,*N*-dimethylcarboxamide to give derivative **72** provided the most potent compound in this series with an IC_{50} value of 56 nM. This result clearly shows that an *N*,*N*-dimethylamide moiety in combination with the appropriate linker to the adamantyl ketone is able to inhibit 11β-HSD1 with high potency as compounds containing this group including **103**, **104**, **62** and **72**, all have IC_{50} values <70 nM.

To establish the structure–activity relationships of the adamantyl ethanone derivatives with various substituents on the phenyl ring, compounds substituted with the carboxylic acid and their corresponding methyl esters were tested. The free acid group may facilitate the aqueous solubility of these hydrophobic molecules. In the adamantyl ethanone ether series (Table 7), it was found that a carboxylic acid group at the *para*

Table 7. In vitro inhibitory activity of phenyl or benzyl carboxylic acids or esters.

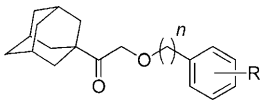

Compd	R	*n*	IC_{50} [nM]
23	*p*-COOMe	0	25 %[a]
40	*p*-COOH	0	74
24	*m*-COOMe	0	78
41	*m*-COOH	0	153
25	*p*-CH_2COOMe	0	2580
59	*p*-CH_2COOH	0	400
32	*p*-COOMe	1	55 %[a]
60	*p*-COOH	1	359

[a] Percent inhibition measured at a concentration of 1 μM.

position, as in compound **40** ($IC_{50}=74$ nM), is much more potent than the corresponding methyl ester analogue **23** (25 % at 1 μM). However, upon moving the methyl ester to the *meta* position to give compound **24**, the activity is regained with an IC_{50} value of 78 nM. This is in agreement with the finding in the benzamide series where hydrophobic interactions are preferred in the *meta* position. The free acid analogue **41** was twofold less potent than **24** and retained activity with an IC_{50} value of 153 nM. However, extending the chain length to give added flexibility, as in compounds **25** and **59**, or extra flexibility in the linker (i.e., compounds **32** and **60**) did not improve the activity. The two free acid derivatives **59** and **60** with extended side chains exhibited moderate inhibition of 11β-HSD1 with IC_{50} values in the 300–400 nM range.

The effects of hydrophobic substituents with different size and electronic properties on the phenyl ring were investigated (Table 8 and Table 9). Compounds with an ethanone ether linker attached directly to the phenyl ring gave only moderately active compounds in the mid to low micromolar range irrespective of the size and electronic properties of the substituents (Table 8). With a sulfide, sulfoxide or sulfone linker in combination with a series of *para*-substituents in the phenyl ring, moderate inhibition of 11β-HSD1 was observed (Table 8). Compounds with nanomolar activity included the *para*-chloro-sulfide-linked analogue **76**, the *para*-methyl-sulfoxide derivative **86** and the *para*-methyl-sulfone **94**, with IC_{50} values of 810 nM, 443 nM and 668 nM, respectively.

Considering the more flexible ethanone ether linker containing an extra methylene unit, it was discovered that the majority of compounds with hydrophobic or aromatic substitutions on the phenyl ring only exhibited weak inhibition of 11β-HSD1,

Table 8. In vitro inhibitory activity of benzene derivatives.

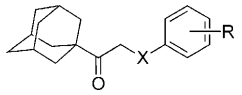

Compd	X	R	IC_{50} [nM]
26	O	*p*-Ph	4900
27	O	*p*-CF_3	5236
28	O	*m*-CF_3	46%[a]
29	O	*p*-Cl	1000
30	O	*p*-Me	2510
31	O	*m*,*p*-di-OMe	9379
76	S	*p*-Cl	810
77	S	*p*-Me	6720
85	SO	*p*-Cl	1438
86	SO	*p*-Me	443
93	SO_2	*p*-Cl	56%[a]
94	SO_2	*p*-Me	668

[a] Percent inhibition measured at a concentration of 1 μM.

especially for compounds with substituents such as phenyl and trifluoromethyl (compounds **33**, **34**, **35**; Table 9). However, the *para*-methoxy and *meta*-*para*-dimethoxy derivatives **37** and **38** showed good inhibition of 11β-HSD1 with IC_{50} values around 300 nM. When replacing the ether linker with a thioether, as in compounds **78**–**82**, only weak inhibition of 11β-HSD1 was achieved.

However, when the ethanone ether linker was replaced with ethanone sulfoxide or sulfone, as in compounds **88**–**99**, some interesting activities were observed. Again, in general, compounds with bulky alkyl substituents in the phenyl ring were only weakly active at inhibiting 11β-HSD1. The *para*-chlorophenyl derivative **87**, with a sulfoxide linker, had an activity sixfold greater than the analogous shorter linker compound **85**, and was a potent inhibitor. The *ortho*-*para*-dichlorophenyl sulfone **99** also exhibited high activity with an IC_{50} value of 171 nM. The most active compounds in these series are **88** (IC_{50} = 122 nM) and **96** (IC_{50} = 128 nM), with an *ortho*-chloro substituent on the phenyl ring and a longer ethanone sulfoxide or sulfone linker, respectively. These are novel, potent inhibitors of 11β-HSD1. The above results indicate that the sulfoxide and sulfone linkers may not only change the geometry of the molecule, but may also interact as hydrogen-bond acceptors with amino acid residues in the active site of 11β-HSD1. Both of these effects would improve the binding of the compounds to 11β-HSD1 through hydrophobic and a network of hydrogen bonding interactions. The results from Tables 8 and 9 indicate that, with the appropriate linker and substitution in the phenyl ring in these adamantyl ketone series, potent inhibition of 11β-HSD1 can be achieved.

Table 9. In vitro inhibitory activity of substituted benzene derivatives with an extended linker.

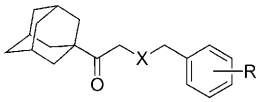

Compd	X	R	IC_{50} [nM]
33	O	*p*-Ph	38%[a]
34	O	*p*-CF_3	35%[a]
35	O	*m*-CF_3	31%[a]
36	O	*p*-Me	2069
37	O	*p*-OMe	296
38	O	*m*,*p*-di-OMe	339
39	O	*p*-Cl	53%[a]
78	S	*p*-Cl	74%[a]
79	S	*o*-Cl	24%[a]
80	S	*m*-Me	26%[a]
81	S	*p*-*t*Bu	68%[a]
82	S	*o*,*p*-di-Cl	68%[a]
87	SO	*p*-Cl	231
88	SO	*o*-Cl	122
89	SO	*p*-*t*Bu	60%[a]
90	SO	*o*,*p*-di-Cl	2975
95	SO_2	*p*-Cl	1350
96	SO_2	*o*-Cl	128
97	SO_2	*m*-Me	45%[a]
98	SO_2	*p*-*t*Bu	2017
99	SO_2	*o*,*p*-di-Cl	171

[a] Percent inhibition measured at a concentration of 1 μM.

Selected compounds from the adamantyl ethanone series were also tested for their selectivity towards 11β-HSD2 and 17β-HSD1, and the results indicated that they did not inhibit these enzymes.

Metabolic stability and CYP450 inhibition studies

A selection of potent compounds (**62**, **72**, **92** and **103**), with IC_{50} values in the 50–70 nM range, was evaluated on human liver microsomes in order to determine their metabolic stability. The results shown in Table 10 represent the remaining quantity of each compound after 30 min incubation, the half-life, the intrinsic clearance and the number of metabolites, as measured by HPLC.

Table 10. Metabolism studies in human liver microsomes.[a]

Compd	Remaining compd [%][b]	$t_{1/2}$ [min]	CL_{int} [μL min^{-1} mg^{-1}]	Metabolites[c]
62	92	67	9.5	0
72	87	59	11	0
92	11	11	73	4
103	50	27	24	2

[a] The parent compound was incubated at 37 °C with human liver microsomes in the presence of the cofactor NADPH for 40 min. Evaluation of disappearance of parent compound and identification of metabolites was performed using HPLC. [b] The amount of compound remaining after 30 min. [c] The number of metabolites detected.

Compound **92**, with an ethanone sulfone linker attached to the 4-acetamidophenyl group, was rapidly metabolised, with only 11% of the original compound left after 30 min, and had a half-life of 11 min; four metabolites were detected by HPLC. The clearance rate of this compound is also high at 73 μL min^{-1} mg^{-1}. Compound **103**, with an ethanone sulfoxide linker, exhibited improved metabolic stability relative to **92**,

with 50% of the compound remaining after 30 min. However, with a half-life of <30 min, two metabolites detected from the microsomal incubation and a clearance rate of 24 $\mu L\,min^{-1}\,mg^{-1}$, this compound is metabolised relatively quickly. On the other hand, compounds **62** and **72**, with an ethanone ether linker, displayed greatly enhanced metabolic stability with ~90% of the compound remaining after 30 min incubation, no metabolites detected by HPLC, a half-life of 1 h and an intrinsic clearance of ~10 $\mu L\,min^{-1}\,mg^{-1}$. These results show that, with the combination of a suitable linker and phenyl acetamide or benzamide substitution, the adamantyl ketone group in **62** and **72** is resistant to metabolism. These compounds show properties worthy of further preclinical studies.

Based on their inhibitory activity against 11β-HSD1 and other properties, compounds **62**, **72** and **103** were selected, and their inhibition of key human cytochrome P450 enzymes (1A2, 2C9, 2C19, 2D6, 3A4-BFC and 3A4-BQ) was examined (Table 11). Compound **72** showed only very weak inhibitory activity against all CYP450 enzymes used in the assay, with IC_{50} values of >100 μM (1A2), >100 μM (2C9), 20 μM (2C19), >100 μM (2D6), 22 μM (3A4-BFC) and 86 μM (3A4-BQ). Although showing no inhibition for 1A2 and 2D6, **62** exhibited some inhibition at a concentration of 10 μM for 2C9 (93%), 2C19 (83%), 3A4-BFC (92%) and 3A4-BQ (51%). Similarly, compound **103** also showed some inhibition at a concentration of 10 μM for 2C19 (71%), 3A4-BFC (100%) and 3A4-BQ (40%). Compound **72** has the best overall profile on both metabolic stability and CYP inhibition.

Table 11. Inhibition of human cytochrome P450 enzymes.

CYP450	Compd **62** [%][a]	Compd **72** (IC_{50} [μM])	Compd **103** [%][a]
1A2	0	>100	0
2C9	93	>100	0
2C19	83	20	71
2D6	0	>100	0
3A4-BFC	92	22	100
3A4-BQ	51	86	40

[a] Percent inhibition measured at a concentration of 10 μM.

Molecular modelling: docking studies

Fourteen of the publicly available crystal structures of human 11β-HSD1 (1XU7,[49] 1XU9,[49] 2BEL, 2ILT,[43] 2IRW,[50] 2RBE,[51] 3BYZ,[52] 3BZU,[53] 3CH6,[54] 3CZR,[55] 3D3E,[56] 3D4N,[56] 3D5Q,[57] 3EY4[44] and 3FRJ[58]) were superimposed to determine the shape, volume and flexibility of the substrate binding site. The NADP(H) molecules from all fourteen structures were found to be superimposable—the different inhibitors have little influence on the structure of the protein around the NADP(H). In Figure 1, all the inhibitor atoms to the right of the vertical black line are in the hydrophobic cortisone (substrate) binding pocket. The atoms to the left of the line are on the surface of the protein exposed to the surrounding solvent.

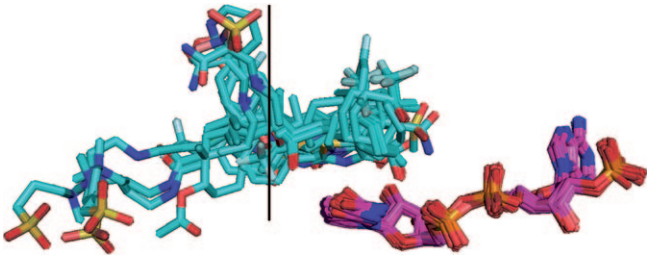

Figure 1. Superimposition of inhibitors and NADP(H) from fourteen human 11β-HSD1 crystal structures.

Figure 2 shows the main chain atoms of the walls of the substrate binding site, but not the atoms at the base of the pocket containing the catalytic residues. For clarity, only the backbone atoms of the superimposed structures are depicted to demonstrate the backbone variability. Looking from the surface of the protein into the substrate binding site, residues Ala 223–Ala 236 on the right and Lys 174–Val 180 on the left form the walls of the binding site. If these two walls of the binding site are static, access to the space between the two walls is limited, and it is unlikely that an inhibitor would be able to access the cortisone binding pocket. However, as shown by the variable conformation of the wall on the right, the two walls of the pocket are probably hinged so that they are able to move apart to allow the cortisone (or inhibitor) into the pocket. This flexibility suggests that bulkier inhibitors may be accommodated in the binding site. 2-(*N*-Morpholino)-ethanesulfonic acid (MES; buff-coloured molecule in Figures 1 and 2) does not lie in the substrate binding site; it is not an inhibitor but a molecule from the crystallisation buffer that lies on the surface of the protein. This shows that inhibitors may

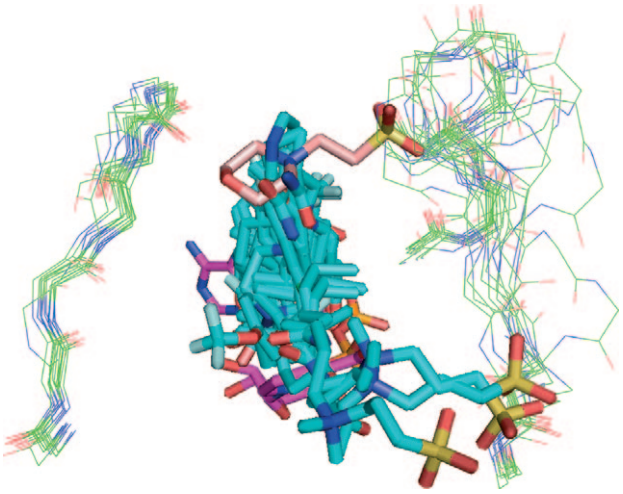

Figure 2. Superimposition of binding site residues of 11β-HSD1 crystal structures.

be able to exploit the area occupied by this molecule to increase potency or selectivity and solubility.

To evaluate which X-ray crystal structure is the most suitable for use in docking studies for our ligands, cortisone and compound **62** were docked, using the GOLD docking program (version 4.1), into all fourteen crystal structures in the presence of the cofactor. Based on the docked poses and the docking scores, we found that the 2ILT, 2IRW and 3CH6 structures were the most suitable for docking studies using our current pharmacophore. The identification of the 2ILT and 2IRW structures as suitable for docking studies was not too surprising as both contain a ligand with a bulky adamantyl group. However, the reason the 3CH6 structure was identified is less clear; in terms of the structure of the substrate binding site, it is very similar to the 2ILT and 2IRW structures. Ligands from the adamantyl ethanone series were chosen and docked into the 2ILT crystal structure with the binding site defined as a sphere of 10 Å radius around the centroid of the ligand in the 2ILT structure. Each ligand was docked 25 times. The GoldScore scoring function was used to rank the ligands in order of fitness.

Figure 3 shows the best docking solutions for both compound **102** and **104**; these predicted binding conformations have the adamantyl part close to the nicotinamide group of

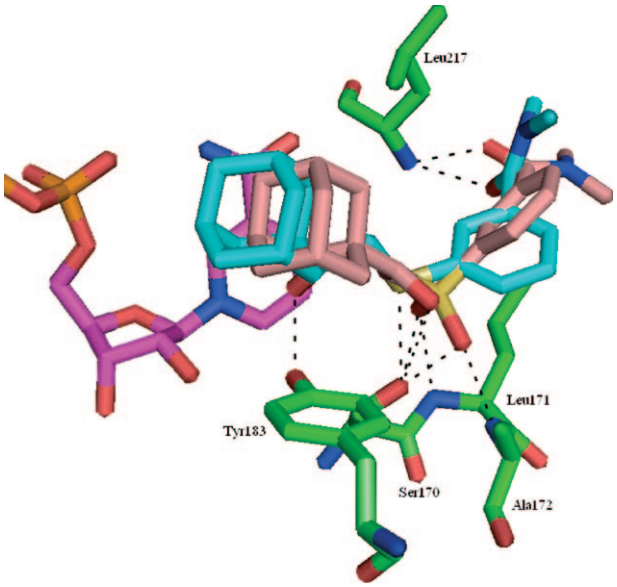

Figure 3. Docking solutions for compounds **102** (in cyan) and **104** (in buff).

the cofactor, fitting tightly into the lipophilic pocket, which is made up of the residues Leu 126, Ile 230, Val 227, Leu 217, Ala 223 and Val 180. The ketone moiety of compound **104** forms a hydrogen bond with the catalytic residue Tyr 183, which is 2.5 Å away. Furthermore, the bridging sulfone group is also in a good position to accept hydrogen bonds from Ser 170 with either oxygen at distances of 2.33 Å and 2.40 Å away as depicted. In addition, Leu 171 and Ala 172, being 2.97 Å and 3.07 Å, respectively, away from a sulfone oxygen of **104**, may also form hydrogen bonding interactions. For compound **102**, it is the bridging sulfur atom rather than the carbonyl group that forms a hydrogen bond acceptor interaction with Ser 170, 2.87 Å away. In both cases, the carbonyl moiety of the acetamide group can accept a hydrogen bond from the backbone NH of Leu 217 being 2.36 Å and 2.39 Å away from **102** and **104**, respectively.

The effects of the *N*-methylacetamide side chain of **61** or the *N*-dimethylacetamide of **62** on the proposed binding mode of the molecules were studied (Figure 4). Both ligands

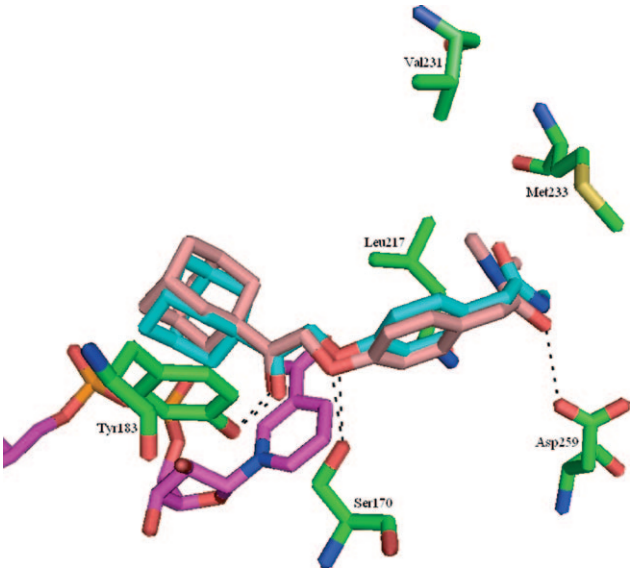

Figure 4. Docking solutions of compounds **61** (in cyan) and **62** (in buff).

are predicted to bind in a way that orients the adamantyl group towards the cofactor, but the direction of the acetamide moiety differs slightly between the two, with the amide carbonyl groups pointing in different directions. The dimethylacetamide moiety of **62** occupies a hydrophobic pocket formed by residues Leu 217, Val 231 and Met 233. The methyl group of the methylacetamide of **61** also fits into this pocket, but the rotation of the carbonyl enables the methylacetamide NH group to form an added hydrogen bond to Asp 259, 3.67 Å away. The carbonyl moiety in both compounds **61** and **62**, being a distance of 2.25 Å and 2.43 Å, respectively, from the catalytic Tyr 183 residue, are likely able to act as hydrogen-bond acceptors. In addition, the ether oxygen in the linker in both compounds **61** and **62** can form a similar hydrogen-bond acceptor interaction with Ser 170 in the active site, being 3.00 Å and 2.67 Å away from this residue, respectively.

With the extended linker system, compound **71** showed some interesting docking modes (Figure 5). The highest scoring solution of **71** does not orient the adamantyl group in the same way as the other ligands examined here. In this proposed binding mode, the adamantyl group is positioned away from the cofactor, and the phenyl ring sits in the hydrophobic pocket near NADP. However, the fourth best solution for **71** has the 'normal' orientation, that is, with the adamantyl group positioned near the cofactor. Compound **71** is 4.5 times less active than **72** and the possibility that this ligand could adopt

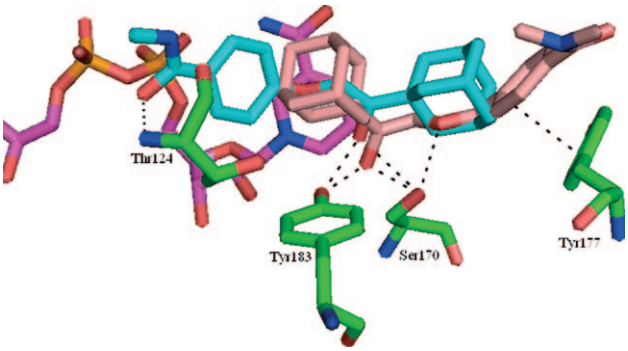

Figure 5. Docking solutions of compounds **71** (in cyan) and **72** (in buff).

two different binding modes could play a part in this. The dimethylacetamide moiety in **72** could play a role in helping the ligand lock itself into this specific binding mode by fitting comfortably into a pocket formed by Leu 126, Pro 178, Met 179, Val 180, Val 227, Val 231 and Met 233. In this orientation, the phenyl ring stacks with the ring of Tyr 177 at a distance of 3.15 Å.

Conclusions

In summary, we report the discovery of adamantyl ethanone derivatives as novel, potent, inhibitors of human 11β-HSD1. A number of compounds were identified with IC_{50} values in the range of 50–70 nM when evaluated on a HEK-293 cell line stably transfected with the *HSD11B1* gene. Potent compounds in these novel series are inactive on human 11β-HSD2 and selected compounds are also inactive on human 17β-HSD1.

The structure–activity relationship studies indicate that an adamantyl ethanone tethered to a substituted phenyl ring through an oxygen, sulfur, sulfoxide or sulfone linker constitutes a suitable pharmacophore for the inhibition of human 11β-HSD1. The linker geometry, side chain size and orientation play a key role in determining the inhibitory properties of the molecules. Molecular modelling of the potent compounds using a crystal structure of human 11β-HSD1 predicted how these molecules may interact with the enzyme and cofactor. The ketone group in the linker is proposed to play a key role, interacting with residues Tyr 183 and Ser 170 in the catalytic region. The mechanistic study from Wyeth suggested that a known 11β-HSD1 inhibitor with a β-keto sulfone linker is a substrate of the enzyme.[59] Our compounds with a ketone group in the same approximate region may also act as substrates; however, we have not tested this hypothesis.

The most potent compound, **72**, exhibited an IC_{50} value of 56 nM for 11β-HSD1 and was metabolically stable upon human liver microsomal incubation with a half-life of 59 min and an intrinsic clearance of 11 $\mu L\,min^{-1}\,mg^{-1}$. Furthermore, compound **72** showed very weak activity against key human CYP450 enzymes and therefore is regarded as a candidate worthy of further preclinical investigation.

Experimental Section

General methods

All chemicals were purchased from either Aldrich Chemical Co. (Gillingham, UK) or Alfa Aesar (Heysham, UK). All organic solvents of AR grade were supplied by Fisher Scientific (Loughborough, UK). Melting points were determined using a Stanford Research Systems Optimelt and are uncorrected. Target compounds in solid form were crystallised from CH_2Cl_2/EtOAc. Thin layer chromatography (TLC) was performed on precoated aluminium plates (Merck, silica gel 60 F_{254}). Product spots were visualised either by UV irradiation at 254 nm and by staining with 5% *w/v* molybdophosphoric acid in EtOH, followed by heating. Flash column chromatography was performed on prepacked columns (Isolute) and gradient elution (solvents indicated in text) on a Flashmaster II system (Biotage). ^{1}H NMR spectra were recorded with a Jeol Delta 270 MHz. Chemical shifts (δ) are reported in parts per million (ppm) relative to tetramethylsilane (TMS) as an internal standard. LC–MS spectra were performed on a Waters 2790 machine with Waters Symmetry C18 column (packing: 3.5 μm, 4.6 mm × 75 mm) eluting with 10% H_2O/CH_3OH (1 mL min^{-1}), and detected with a ZQ MicroMass spectrometer and PDA detector using Atmospheric Pressure Chemical Ionisation (APCI) or Electrospray Ionisation (ESI). High resolution mass spectra were recorded on a Bruker MicroTOF with ESI or at the EPSRC National Mass Spectrometry service, Swansea with the FAB-MS using *m*-nitrobenzyl alcohol (NBA) as the matrix. HPLC was undertaken using a Waters 717 machine with Autosampler and PDA detector. The column used was a Waters Symmetry C18 (packing: 3.5 μm, 4.6 mm × 150 mm) with an isocratic mobile phase consisting of H_2O/CH_3CN with a flow rate of 1.0 mL min^{-1}.

11β-HSD1 scintillation proximity assay (SPA) protocol: human cell based assay[60]

Nontransfected HEK293 cells lack endogenous 11β-HSD1 activity, and this cell line has been shown to be a suitable system for evaluating 11β-HSD1 activity after being transfected with the plasmid for expression of 11β-HSD1 or 11β-HSD2. The enzyme activity was determined by measuring the amount of tritiated product by using a scintillation proximity assay (SPA). The high-throughput cell-based assays were conducted on the human 11β-HSD1 transfected HEK293 cell line with an SPA. The activity of 11β-HSD1 was measured in whole HEK293 cells stably transfected with the *HSD11B1* gene using modified literature protocols. Cells were incubated in 96-well microplates in the presence of tritiated substrate, and the assay plates contained internal high and low controls to allow calculation of the percent inhibition. Each well of a 96-well culture plate was seeded with HEK293/HSD11B1 cells in 100 μL medium. When the cells were 80% confluent, the medium was removed from each well and then 100 μL of fresh, serum-free, medium containing [^{3}H]cortisone and test compound in 1% DMSO were added to each well. The control wells were also dispensed. The high control wells did not contain compound, while low controls did not contain cells. The plate was incubated at 37 °C for the required time period, after which, 50 μL of media was removed from each well and transferred to a microplate containing 100 μL of a pre-incubated mixture of anticortisol antibody and SPA bead. The mixture was incubated with gentle shaking until equilibrium was reached, before transferring to a scintillation counter to establish the enzyme activity in each sample.

Docking study procedure

Selected ligands were docked into the 11β-HSD1 protein X-ray crystal structure (PDB: 2ILT) using the GOLD docking program, version 4.1 with default settings in the presence of the cofactor. The binding site was defined as a sphere of 10 Å radius around the centroid of the ligand in the 2ILT crystal structure. Each ligand was docked 25 times. The GoldScore scoring function was used to rank the ligands in order of fitness.

Method A: Synthesis of ethanone amino linker compounds 11–14

A solution of aryl bromomethyl ketone or 1-adamantyl bromomethyl ketone (1 mmol) in ethanol or CH_3CN (10 mL) was treated with K_2CO_3 (100 mg), followed by the corresponding amine (1 mmol). The mixture was stirred at RT under nitrogen, and monitored by TLC. After completion, the mixture was partitioned between EtOAc and 5% aq $NaHCO_3$. The organic phase was washed with brine, dried over Na_2SO_4 and concentrated in vacuo to give the crude product. Purification using flash chromatography (hexane/EtOAc; gradient elution) yielded the target compound (yield 40–70%).

1-(4-Chlorophenyl)-2-(2-methylbenzo[*d*]thiazol-5-ylamino)ethanone (11): A light yellow solid (90 mg); mp: 172–174 °C; ^{1}H NMR (270 MHz, $CDCl_3$): δ = 2.79 (s, 3H), 4.64 (d, J = 4.5 Hz, 2H), 5.00 (t, J = 4.4 Hz, 1H), 6.83 (dd, J = 8.6, 2.2 Hz, 1H), 7.18 (d, J = 2.2 Hz, 1H), 7.50 (dt, J = 8.6, 1.8 Hz, 2H), 7.59 (d, J = 8.7 Hz, 1H) and 7.96 (dt, J = 8.4, 1.8 Hz, 2H); LC–MS (APCI) m/z: 315 $[M-H]^-$; HRMS (FAB) m/z $[M+H]^+$ calcd for $C_{16}H_{14}ClN_2OS$: 317.0515, found: 317.0504; HPLC: t_R = 2.52 min (98%) in 20% H_2O/CH_3CN.

1-(2,4-Dichlorophenyl)-2-(2-methylbenzo[*d*]thiazol-5-ylamino)-ethanone (12): A yellow solid (168 mg); mp: 125–127 °C; ^{1}H NMR (270 MHz, $CDCl_3$): δ = 2.78 (s, 3H), 4.61 (brs, 2H), 4.91 (brs, 1H), 6.78 (dd, J = 8.8, 2.6 Hz, 1H), 7.13 (d, J = 2.2 Hz, 1H), 7.36 (dd, J = 8.4, 2.0 Hz, 1H), 7.50 (d, J = 2.0 Hz, 1H), 7.57 (d, J = 8.7 Hz, 1H) and 7.67 (d, J = 8.4 Hz, 1H); LC–MS (APCI) m/z: 349 $[M-H]^-$; HRMS (FAB) m/z $[M+H]^+$ calcd for $C_{16}H_{13}Cl_2N_2OS$: 351.0126, found: 351.0109; HPLC: t_R = 2.58 min (98%) in 20% H_2O/CH_3CN.

1-Adamantan-1-yl-2-(2-methylbenzothiazol-5-ylamino)ethanone (13): An off-white solid (185 mg); mp: 133–136 °C; ^{1}H NMR (270 MHz, $CDCl_3$): δ = 1.69 (m, 6H), 1.84 (d, J = 2.7 Hz, 6H), 2.02 (brs, 3H), 2.71 (s, 3H), 4.06 (s, 2H), 4.75 (brs, 1H), 6.68 (dd, J = 8.6, 2.4 Hz, 1H), 7.03 (d, J = 2.2 Hz, 1H), 7.48 (d, J = 8.8 Hz, 1H); LC–MS (APCI) m/z: 341 $[M+H]^+$; HRMS (FAB) m/z $[M+H]^+$ calcd for $C_{20}H_{25}N_2OS$: 341.1687, found: 341.1683; HPLC: t_R = 3.53 min (99%) in 20% H_2O/CH_3CN.

***N*-[4-(2-Adamantan-1-yl-2-oxoethylamino)phenyl]acetamide (14)**: A white solid (222 mg); mp: 156–158 °C; ^{1}H NMR (270 MHz, $CDCl_3$): δ = 1.66–1.75 (m, 6H), 1.87 (d, J = 2.8 Hz, 6H), 2.07 (brs, 3H), 2.12 (s, 3H), 4.04 (s, 2H), 4.63 (brs, 1H), 6.57 (dd, J = 7.1, 1.9 Hz, 2H), 6.99 (brs, 1H), 7.28 (dd, J = 7.2, 1.9 Hz, 2H); LC–MS (APCI) m/z: 327 $[M+H]^+$; HRMS (FAB) m/z $[M+H]^+$ calcd for $C_{20}H_{27}N_2O_2$ 327.2073, found: 327.2075; HPLC: t_R = 4.93 min (98%) in 10% H_2O/CH_3CN.

Method B: Synthesis of ethanone ether linker compounds 15–31

A solution of 1-adamantyl bromomethyl ketone (257 mg, 1 mmol) in acetone or DMF (10 mL) was treated with K_2CO_3 (276 mg, 2 mmol), followed by the corresponding phenol (1 mmol). The mixture was stirred at RT under nitrogen, and monitored by TLC. After completion, the mixture was partitioned between EtOAc and brine. The organic phase was washed with brine, dried over Na_2SO_4 and concentrated in vacuo to give the crude product. Purification using flash chromatography (hexane/EtOAc or CH_2Cl_2/EtOAc; gradient elution) yielded the target compound (yield 37–100%).

1-Adamantan-1-yl-2-(2-methylbenzothiazol-5-yloxy)ethanone (15): A white solid (341 mg, 100%); mp: 123–124.5 °C; ^{1}H NMR (270 MHz, $CDCl_3$): δ = 1.71–1.79 (6H, m), 1.93 (brd, J = 3.0 Hz, 6H), 2.04–2.11 (m, 3H), 2.78 (s, 3H), 4.94 (s, 2H), 7.04 (dd, J = 8.8, 2.5 Hz, 1H), 7.28 (d, J = 2.5 Hz, 1H), 7.66 (d, J = 8.9 Hz, 1H); LC–MS (APCI) m/z: 342.4 $[M+H]^+$; HRMS (FAB) m/z $[M+H]^+$ calcd for $C_{20}H_{24}NO_2S$: 342.1522, found: 342.1521; HPLC: t_R = 18.7 min (>99%) in 30% H_2O/CH_3CN.

***N*-[4-(2-Adamantan-1-yl-2-oxoethoxy)phenyl]acetamide (16)**: A white crystalline solid (281 mg, 86%); mp: 177–178 °C; ^{1}H NMR (270 MHz, $CDCl_3$): δ = 1.66–1.82 (m, 6H), 1.90 (d, J = 2.7 Hz, 6H), 2.07 (brs, 3H), 2.13 (s, 3H), 4.82 (s, 2H), 6.80 (dt, J = 8.9, 2.2 Hz, 2H), 7.13 (brs, 1H), 7.36 (dt, J = 9.0, 2.3 Hz, 2H); LC–MS (APCI) m/z: 326 $[M-H]^-$; HRMS (FAB) m/z $[M+Na]^+$ calcd for $C_{20}H_{25}NO_3Na$: 350.1732, found: 350.1720; HPLC: t_R = 2.45 min (>99%) in 10% H_2O/CH_3CN.

***N*-[3-(2-Adamantan-1-yl-2-oxoethoxy)phenyl]acetamide (17)**: A white solid (300 mg, 92%); mp: 136–137 °C; ^{1}H NMR (270 MHz, $CDCl_3$): δ = 1.68–1.79 (m, 6H), 1.91 (d, J = 2.7 Hz, 6H), 2.06 (brs, 3H), 2.15 (s, 3H), 4.86 (s, 2H), 6.63 (dd, J = 8.3, 2.2 Hz, 1H), 6.90 (dd, J = 8.2, 2.2 Hz, 1H), 7.14–7.20 (m, 2H), 7.30 (t, J = 2.7 Hz, 1H); LC–MS (ESI) m/z 326 $[M-H]^-$; HRMS (ESI) m/z $[M+Na]^+$ calcd for $C_{20}H_{25}NO_3Na$: 350.1732, found: 350.1704; HPLC: t_R = 2.18 min (99%) in 10% H_2O/CH_3CN.

***N*-[4-(2-Adamantan-1-yl-2-oxoethoxy)-2-methyl-phenyl]acetamide (18)**: An off-white amorphous solid (158 mg, 46%); mp: 201–204 °C; ^{1}H NMR (270 MHz, $CDCl_3$): δ = 1.68–1.82 (m, 6H), 1.90 (d, J = 2.7 Hz, 6H), 2.07 (brs, 3H), 2.16 (s, 3H), 2.20 (s, 3H), 4.80 (s, 2H), 6.65 (dd, J = 8.8, 2.9 Hz, 1H), 6.72 (d, J = 3.0 Hz, 1H), 6.83 (brs, 1H), 7.17 (d, J = 8.7 Hz, 1H); LC–MS (APCI) m/z: 340 $[M-H]^-$; HRMS (FAB) m/z $[M+Na]^+$ calcd for $C_{21}H_{27}NO_3Na$: 364.1889, found: 364.1868; HPLC: t_R = 1.78 min (99%) in 10% H_2O/CH_3CN.

***N*-[4-(2-Adamantan-1-yl-2-oxoethoxy)-2-chloro-phenyl]acetamide (19)**: A white solid (280 mg, 77%); mp: 204–206 °C; ^{1}H NMR (270 MHz, $CDCl_3$): δ = 1.65–1.80 (m, 6H), 1.90 (d, J = 2.8 Hz, 6H), 2.07 (brs, 3H), 2.20 (s, 3H), 4.81 (s, 2H), 6.76 (dd, J = 9.0, 3.0 Hz, 1H), 7.24 (d, J = 2.9 Hz, 1H), 7.38 (brs, 1H), 8.17 (d, J = 9.0 Hz, 1H); LC–MS (APCI) m/z: 360 $[M-H]^-$; HRMS (FAB) m/z $[M+Na]^+$ calcd for $C_{20}H_{24}ClNO_3Na$: 384.1342, found: 384.1320; HPLC: t_R = 1.92 min (99%) in 10% H_2O/CH_3CN.

***N*-[4-(2-Adamantan-1-yl-2-oxoethoxy)-3-chloro-phenyl]acetamide (20)**: A white solid (330 mg, 91%); mp: 227–228.5 °C; ^{1}H NMR (270 MHz, $CDCl_3$): δ = 1.68–1.78 (m, 6H), 1.91 (d, J = 2.7 Hz, 6H), 2.00 (brs, 3H), 2.14 (s, 3H), 4.89 (s, 2H), 6.53 (d, J = 8.9 Hz, 1H), 7.15 (brs, 1H), 7.31 (dd, J = 8.9, 2.7 Hz, 1H), 7.49 (d, J = 2.8 Hz, 1H); LC–MS (APCI) m/z: 360 $[M-H]^-$; HRMS (ESI) m/z $[M+Na]^+$ calcd for $C_{20}H_{24}ClNO_3Na$: 384.1342, found: 384.1328; HPLC: t_R = 2.22 min (>99%) in 10% H_2O/CH_3CN.

***N*-[4-(2-Adamantan-1-yl-2-oxoethoxy)-2-fluoro-phenyl]acetamide (21)**: A white solid (230 mg, 67%); mp: 191–192.5 °C; ^{1}H NMR (270 MHz, $CDCl_3$): δ = 1.65–1.80 (m, 6H), 1.90 (d, J = 2.8 Hz, 6H), 2.07 (brs, 3H), 2.18 (s, 3H), 4.81 (s, 2H), 6.55–6.70 (m, 2H), 7.14 (brs, 1H), 8.08 (t, J = 8.9 Hz, 1H); LC–MS (APCI) m/z: 344 $[M-H]^-$;

HRMS (FAB) *m/z* $[M+Na]^+$ calcd for $C_{20}H_{24}FNO_3Na$: 368.1638, found: 368.1619; HPLC: $t_R = 1.79$ min (99%) in 10% H_2O/CH_3CN.

***N*-[4-(2-Adamantan-1-yl-2-oxoethoxy)-3-methyl-phenyl]acetamide (22)**: A white solid (255 mg, 75%); mp: 201–202.5 °C; ^1H NMR (270 MHz, $CDCl_3$): $\delta = 1.58$–1.75 (m, 6H), 1.91 (d, $J = 2.7$ Hz, 6H), 2.06 (brs, 3H), 2.13 (s, 3H), 2.26 (s, 3H), 4.82 (s, 2H), 6.54 (d, $J = 8.7$ Hz, 1H), 7.02 (brs, 1H), 7.17 (d, $J = 2.4$ Hz, 1H), 7.26 (dd, $J = 8.7$, 2.5 Hz, 1H); LC–MS (APCI) *m/z*: 340 $[M-H]^-$; HRMS (ESI) *m/z* $[M+H]^+$ calcd for $C_{21}H_{28}NO_3$: 342.2069, found: 342.2052; HPLC: $t_R = 2.89$ min (99%) in 30% H_2O/CH_3CN.

4-(2-Adamantan-1-yl-2-oxoethoxy)benzoic acid methyl ester (23): A white solid (122 mg, 37%); mp: 128–129 °C; ^1H NMR (270 MHz, $CDCl_3$): $\delta = 1.68$–1.83 (m, 6H), 1.91 (d, $J = 2.7$ Hz, 6H), 2.08 (brs, 3H), 3.87 (s, 3H), 4.90 (s, 2H), 6.85 (dt, $J = 9.1$, 2.7 Hz, 2H), 7.96 (dt, $J = 8.9$, 2.7 Hz, 2H); LC–MS (APCI) *m/z*: 329 $[M+H]^+$; HRMS (FAB) *m/z* $[M+H]^+$ calcd for $C_{20}H_{25}O_4$: 329.1747, found: 329.1736; HPLC: $t_R = 2.39$ min (98%) in 10% H_2O/CH_3CN.

3-(2-Adamantan-1-yl-2-oxoethoxy)benzoic acid methyl ester (24): A white solid (326 mg, 99%); mp: 84–85 °C; ^1H NMR (270 MHz, $CDCl_3$): $\delta = 1.68$–1.82 (m, 6H), 1.92 (d, $J = 2.9$ Hz, 6H), 2.08 (brs, 3H), 3.89 (s, 3H), 4.90 (s, 2H), 7.11 (ddd, $J = 8.4$, 2.7, 1.0 Hz, 1H), 7.33 (t app, $J = 7.9$ Hz, 1H), 7.46 (dd, $J = 2.7$, 1.5 Hz, 1H), 7.63 (dt, $J = 6.5$, 1.2 Hz, 1H); LC–MS (APCI) *m/z*: 327 $[M-H]^-$; HRMS (FAB) *m/z* $[M+H]^+$ calcd for $C_{20}H_{25}O_4$: 329.1747, found: 329.1746; HPLC: $t_R = 3.05$ min (>99%) in 10% H_2O/CH_3CN.

[4-(2-Adamantan-1-yl-2-oxoethoxy)phenyl]acetic acid methyl ester (25): A white solid (294 mg, 86%); mp: 71–72 °C; ^1H NMR (270 MHz, $CDCl_3$): $\delta = 1.65$–1.85 (m, 6H), 1.90 (d, $J = 2.9$ Hz, 6H), 2.06 (brs, 3H), 3.54 (s, 2H), 3.66 (s, 3H), 4.82 (s, 2H), 6.80 (dt, $J = 8.7$, 2.9 Hz, 2H), 7.16 (dt, $J = 8.7$, 2.9 Hz, 2H); LC–MS (APCI) *m/z*: 341.7 $[M-H]^-$; HRMS (FAB) *m/z* $[M+H]^+$ calcd for $C_{21}H_{27}O_4$: 343.1904, found: 343.1892; HPLC: $t_R = 2.23$ min (98%) in 10% H_2O/CH_3CN.

1-Adamantan-1-yl-2-(biphenyl-4-yloxy)ethanone (26): A white solid (197 mg, 57%); mp: 117–118.5 °C; ^1H NMR (270 MHz, $CDCl_3$): $\delta = 1.70$–1.81 (m, 6H), 1.94 (d, $J = 2.8$ Hz, 6H), 2.08 (brs, 3H), 4.89 (s, 2H), 6.92 (dt, $J = 8.7$, 3.2 Hz, 2H), 7.30 (dt, $J = 7.2$, 1.3 Hz, 1H), 7.37–7.42 (m, 2H), 7.47–7.54 (m, 4H); LC–MS (APCI) *m/z*: 347 $[M+H]^+$; HRMS (FAB) *m/z* $[M+H]^+$ calcd for $C_{24}H_{27}O_2$: 347.2011, found: 347.2002; HPLC: $t_R = 5.25$ min (>99%) in 10% H_2O/CH_3CN.

1-Adamantan-1-yl-2-(4-trifluoromethyl-phenoxy)ethanone (27): A white solid (321 mg, 95%); mp: 78–80 °C; ^1H NMR (270 MHz, $CDCl_3$): $\delta = 1.65$–1.85 (m, 6H), 1.91 (d, $J = 3.0$ Hz, 6H), 2.08 (brs, 3H), 4.90 (s, 2H), 6.88 (d, $J = 8.6$ Hz, 2H), 7.52 (d, $J = 8.6$ Hz, 2H); LC–MS (APCI) *m/z*: 337.0 $[M-H]^-$; HRMS (FAB) *m/z* $[M+H]^+$ calcd for $C_{19}H_{22}F_3O_2$: 339.1566, found: 339.1565; HPLC: $t_R = 3.30$ min (97%) in 10% H_2O/CH_3CN.

1-Adamantan-1-yl-2-(3-trifluoromethyl-phenoxy)ethanone (28): A white solid (337 mg, 99%); mp: 87–92 °C; ^1H NMR (270 MHz, $CDCl_3$): $\delta = 1.65$–1.88 (m, 6H), 1.90 (d, $J = 2.7$ Hz, 6H), 2.07 (brs, 3H), 4.88 (s, 2H), 7.01 (brdd, $J = 8.3$, 2.5 Hz, 1H), 7.05 (brs, 1H), 7.20 (brd, $J = 7.7$ Hz, 1H), 7.36 (t, $J = 8.0$ Hz, 1H); LC–MS (APCI) *m/z*: 337 $[M-H]^-$; HRMS (FAB) *m/z* $[M+H]^+$ calcd for $C_{19}H_{22}F_3O_2$: 339.1566, found: 339.1560; HPLC: $t_R = 3.96$ min (>99%) in 10% H_2O/CH_3CN.

1-Adamantan-1-yl-2-(4-chloro-phenoxy)ethanone (29): A white crystalline solid (243 mg, 80%); mp: 112.5–113.5 °C; ^1H NMR (300 MHz, $CDCl_3$): $\delta = 1.71$–1.83 (m, 6H), 1.93 (d, $J = 2.7$ Hz, 6H), 2.10 (brs, 3H), 4.84 (s, 2H), 6.80 (dt, $J = 8.9$, 2.2 Hz, 2H), 7.23 (dt, $J = 9.0$, 2.2 Hz, 2H); LC–MS (APCI) *m/z*: 305 $[M+H]^+$; HRMS (FAB) *m/z* $[M+H]^+$ calcd for $C_{18}H_{22}ClO_2$: 305.1308, found: 305.1299; HPLC: $t_R = 2.41$ min (>99%) in 4% H_2O/CH_3CN.

1-Adamantan-1-yl-2-p-tolyloxy-ethanone (30): A white crystalline solid (244 mg, 86%); mp 90–91 °C; ^1H NMR (300 MHz, $CDCl_3$): $\delta = 1.71$–1.83 (m, 6H), 1.93 (d, $J = 2.7$ Hz, 6H), 2.09 (brs, 3H), 2.28 (s, 3H), 4.83 (s, 2H), 6.78 (dt, $J = 8.9$, 2.0 Hz, 2H), 7.09 (dt, $J = 8.8$, 2.0 Hz, 2H); LC–MS (APCI) *m/z*: 285 $[M+H]^+$; HRMS (FAB) *m/z* $[M+H]^+$ calcd for $C_{19}H_{25}O_2$: 285.1855, found: 285.1849; HPLC: $t_R = 2.44$ min (>99%) in 4% H_2O/CH_3CN.

1-Adamantan-1-yl-2-(3,4-dimethoxy-phenoxy)ethanone (31): A white crystalline solid (278 mg, 84%); mp: 113.5–114.5 °C; ^1H NMR (270 MHz, $CDCl_3$): $\delta = 1.69$–1.79 (m, 6H), 1.90 (d, $J = 2.8$ Hz, 6H), 2.07 (brs, 3H), 3.81 (s, 3H), 3.83 (s, 3H), 4.79 (s, 2H), 6.27 (dd, $J = 8.9$, 3.0 Hz, 1H), 6.59 (d, $J = 2.8$ Hz, 1H), 6.73 (d, $J = 8.7$ Hz, 1H); LC–MS (APCI) *m/z*: 331 $[M+H]^+$; HRMS (FAB) *m/z* $[M+H]^+$ calcd for $C_{20}H_{27}O_4$: 331.1909, found: 331.1902; HPLC: $t_R = 3.15$ min (>99%) in 10% H_2O/CH_3CN.

Method C: Synthesis of ethanone ether linker compounds 32–37

A suspension of NaH (60% in mineral oil, 1.1 equiv) in dry THF was treated with the alcohol (1.0 equiv) at 0 °C. After stirring for 30 min at 0 °C, 1-adamantyl bromomethyl ketone (1.1 equiv) was added in dry THF. The reaction was stirred for 2 h at 0 °C then allowed to warm to RT overnight. After quenching with water, the mixture was extracted twice with Et_2O, washed with water then brine, dried over $MgSO_4$, and then concentrated in vacuo. The crude product was purified using flash chromatography (hexane/EtOAc or CH_2Cl_2/EtOAc; gradient elution) to yield the target compound (yield 15–43%).

4-(2-Adamantan-1-yl-2-oxoethoxymethyl)benzoic acid methyl ester (32): A white solid (61 mg, 15%); mp: 87–90 °C; ^1H NMR (270 MHz, $CDCl_3$): $\delta = 1.60$–1.79 (m, 6H), 1.80 (d, $J = 2.7$ Hz, 6H), 2.01 (brs, 3H), 3.90 (s, 3H), 4.32 (s, 2H), 4.61 (s, 2H), 7.42 (d, $J = 8.2$ Hz, 2H), 8.00 (d app, $J = 8.4$ Hz, 2H); LC–MS (APCI) *m/z*: 365.5 $[M+Na]^+$; HRMS (FAB) *m/z* $[M+H]^+$ calcd for $C_{21}H_{27}O_4$: 343.1904, found: 343.1897; HPLC: $t_R = 2.20$ min (97%) in 10% H_2O/CH_3CN.

1-Adamantan-1-yl-2-(biphenyl-4-ylmethoxy)ethanone (33): White crystals (81 mg, 43%); mp: 80–82 °C; ^1H NMR (270 MHz, $CDCl_3$): $\delta = 1.79$–1.61 (m, 6H), 1.82 (d app, $J = 3.0$ Hz, 6H), 2.02 (brs, 3H), 4.34 (s, 2H), 4.62 (s, 2H), 7.29–7.37 (m, 1H), 7.39–7.47 (m, 4H), 7.54–7.62 (m, 4H); LC–MS (APCI) *m/z*: 383.58 $[M+Na]^+$; HRMS (FAB) *m/z* $[M+NH_4]^+$ calcd for $C_{24}H_{32}NO_2$: 378.2428, found: 378.2424; HPLC: $t_R = 3.99$ min (>99%) in 10% H_2O/CH_3CN.

1-Adamantan-1-yl-2-(4-trifluoromethylbenzyloxy)ethanone (34): A white solid (88 mg,32%); mp: 108–111 °C; ^1H NMR (270 MHz, $CDCl_3$): $\delta = 1.60$–1.78 (m, 6H), 1.80 (d, $J = 2.5$ Hz, 6H), 2.01 (brs, 3H), 4.34 (s, 2H), 4.60 (s, 2H), 7.47 (d, $J = 8.2$ Hz, 2H), 7.58 (d, $J = 8.3$ Hz, 2H); LC–MS (APCI) *m/z*: 375.2 $[M+Na]^+$; HRMS (FAB) *m/z* $[M+H]^+$ calcd for $C_{20}H_{24}F_3O_2$: 353.1723, found: 353.1710; HPLC: $t_R = 3.94$ min (99%) in 10% H_2O/CH_3CN.

1-Adamantan-1-yl-2-(3-trifluoromethylbenzyloxy)ethanone (35): A yellow solid (30 mg, 15%); mp: 45.5–50 °C; ^1H NMR (270 MHz, $CDCl_3$): $\delta = 1.60$–1.80 (m, 6H), 1.81 (d, $J = 2.7$ Hz, 6H), 2.02 (brs, 3H), 4.36 (s, 2H), 4.60 (s, 2H), 7.43–7.59 (m, 3H), 7.62 (s, 1H); LC–MS (APCI) *m/z*: 375.0 $[M+Na]^+$; HRMS (FAB) *m/z* $[M+H]^+$ calcd for $C_{20}H_{24}F_3O_2$: 353.1723, found: 353.1716; HPLC: $t_R = 4.12$ min (97%) in 10% H_2O/CH_3CN.

1-Adamantan-1-yl-2-(4-methylbenzyloxy)ethanone (36): White crystals (33 mg, 28%); mp: 63–65 °C; ^{1}H NMR (270 MHz, $CDCl_3$): δ = 1.59–1.98 (m, 12H), 2.01 (brs, 3H), 2.33 (s, 3H), 4.27 (s, 2H), 4.53 (s, 2H), 7.11–7.19 (m, 2H), 7.25 (m, 2H); LC–MS (APCI) *m/z*: 299 $[M+H]^+$; HRMS (FAB) *m/z* $[M+NH_4]^+$ calcd for $C_{20}H_{30}NO_2$: 316.2271, found: 316.2270; HPLC: t_R = 9.40 min (>99%) in 10% H_2O/CH_3CN.

1-Adamantan-1-yl-2-(4-methoxy-benzyloxy)ethanone (37): An off-white oil (69 mg, 16%); ^{1}H NMR (270 MHz, $CDCl_3$): δ = 1.60–1.88 (m, 12H), 1.92–2.18 (brs, 3H), 3.80 (s, 3H), 4.25 (s, 2H), 4.49 (s, 2H), 6.86 (d app, *J* = 8.7 Hz, 2H), 7.27 (d app, *J* = 8.4 Hz, 2H); LC–MS (APCI) *m/z*: 337 $[M+Na]^+$; HRMS (FAB) *m/z* $[M+NH_4]^+$ calcd for $C_{20}H_{30}NO_3$: 332.2220 found 332.2222; HPLC: t_R = 7.00 min (>99%) in 10% H_2O/CH_3CN.

1-Adamantan-1-yl-2-(3,4-dimethoxy-benzyloxy)ethanone (38): A solution of 3,4-dimethoxybenzyl alcohol (0.139 mL, 0.97 mmol) and 1-adamantyl bromomethyl ketone (250 mg, 0.97 mmol) in toluene (7 mL) was treated with *t*BuOK (217 mg, 1.94 mmol) at RT and was stirred overnight. The reaction was quenched with water, extracted twice with EtOAc, washed with brine, dried over $MgSO_4$ and concentrated in vacuo. The crude mixture was purified using flash chromatography using a gradient of 0–50% EtOAc in hexane to give the target compound (47 mg, 14%) as white solid; mp 60.5–63.5 °C; ^{1}H NMR (270 MHz, $CDCl_3$): δ = 1.60–1.78 (m, 6H), 1.78 (d, *J* = 2.7 Hz, 6H), 2.00 (brs, 3H), 3.86 (s, 3H), 3.87 (s, 3H), 4.26 (s, 2H), 4.50 (s, 2H), 6.82 (s, 1H), 6.84 (d, *J* = 1.7 Hz, 1H), 6.93 (d, *J* = 1.7 Hz, 1H); LC–MS (APCI) *m/z*: 367 $[M+Na]^+$; HRMS (FAB) *m/z* $[M+Na]^+$ calcd for $C_{21}H_{28}O_4Na$: 367.1880, found: 367.1865; HPLC: t_R = 2.88 min (98%) in 10% H_2O/CH_3CN.

1-Adamantan-1-yl-2-(4-chloro-benzyloxy)ethanone (39): The title compound was synthesised by method C as white solid (52 mg, 21%); mp: 91–92 °C; ^{1}H NMR (270 MHz, $CDCl_3$): δ = 1.58–1.72 (m, 6H), 1.75 (d, *J* = 2.7 Hz, 6H), 2.00 (brs, 3H), 4.20 (s, 2H), 4.48 (s, 2H), 7.25 (s, 4H); LC–MS (APCI) *m/z*: 319 $[M+H]^+$; HRMS (FAB) *m/z* $[M+H]^+$ calcd for $C_{19}H_{24}ClO_2$: 319.1465, found: 319.1460; HPLC: t_R = 4.69 min (98%) in 10% H_2O/CH_3CN.

4-(2-Adamantan-1-yl-2-oxoethoxy)benzoic acid (40): The target compound was prepared by hydrolysis of **23** (100 mg, 0.30 mmol) in MeOH/H_2O (2.5–0.5 mL) with LiOH (38 mg, 1.6 mmol) at RT. A white solid (75 mg, 79%) was obtained; mp: 184–187 °C; ^{1}H NMR (270 MHz, $CDCl_3$): δ = 1.69–1.85 (m, 6H), 1.92 (d, *J* = 2.7 Hz, 6H), 2.08 (brs, 3H), 4.93 (s, 2H), 6.87 (d, *J* = 8.9 Hz, 2H), 8.03 (d, *J* = 8.9 Hz, 2H); LC–MS (APCI) *m/z*: 313 $[M-H]^-$; HRMS (FAB) *m/z* $[M+H]^+$ calcd for $C_{19}H_{23}O_4$: 315.1591, found: 315.1600; HPLC: t_R = 1.28 min (98%) in 10% H_2O/CH_3CN.

3-(2-Adamantan-1-yl-2-oxoethoxy)benzoic acid (41): The target compound was prepared by hydrolysis of **24** (880 mg, 2.67 mmol) in MeOH/H_2O (23–4 mL) with LiOH (337 mg, 8 mmol) at RT. A white solid (797 mg, 99%) was obtained; mp: 153–158.5 °C; ^{1}H NMR (270 MHz, $CDCl_3$): δ = 1.67–1.85 (m, 6H), 1.93 (d, *J* = 2.9 Hz, 6H), 2.09 (brs, 3H), 4.91 (s, 2H), 7.17 (ddd, *J* = 8.4, 2.7, 1.0 Hz, 1H), 7.37 (t app, *J* = 8.2 Hz, 1H), 7.51 (dd, *J* = 2.7, 1.5 Hz, 1H), 7.72 (dt, *J* = 7.9, 1.2 Hz, 1H); LC–MS (APCI) *m/z*: 313 $[M-H]^-$; HRMS (FAB) *m/z* $[M+H]^+$ calcd for $C_{19}H_{23}O_4$: 315.1591, found: 315.1580; HPLC: t_R = 1.21 min (97%) in 10% H_2O/CH_3CN.

Method D: Synthesis of the carboxamide derivatives 42–58

A solution of the carboxylic acid (1.0 equiv) in CH_2Cl_2 (5 mL) was treated with EDCI (1.2 equiv), HOBt (0.5 equiv), Et_3N (1.2 equiv) and DMAP (catalytic amount) at RT. After stirring for 30 min, the amine (1.2 equiv) was added and the reaction mixture was stirred overnight and then extracted twice with CH_2Cl_2. The organic phase was washed with 5% aq $NaHCO_3$ and brine, dried over $MgSO_4$ and then concentrated in vacuo. The crude mixture was purified by flash chromatography with EtOAc/hexane or MeOH/CH_2Cl_2 using gradient elution to give the expected amide (yield 33–88%).

4-(2-Adamantan-1-yl-2-oxoethoxy)benzamide (42): A white solid (33 mg, 33%); mp: 176–179.5 °C; ^{1}H NMR (270 MHz, $CDCl_3$): δ = 1.60–1.82 (m, 6H), 1.91 (d, *J* = 2.2 Hz, 6H), 2.08 (brs, 3H), 4.91 (s, 2H), 5.77 (brs, 1H), 5.99 (brs, 1H), 6.86 (d, *J* = 8.5 Hz, 2H), 7.73 (d, *J* = 8.8 Hz, 2H); LC–MS (APCI) *m/z*: 312 $[M-H]^-$; HRMS (FAB) *m/z* $[M+H]^+$ calcd for $C_{19}H_{24}NO_3$: 314.1751, found: 314.1749; HPLC: t_R = 2.00 min (98%) in 10% H_2O/CH_3CN.

4-(2-Adamantan-1-yl-2-oxoethoxy)-*N*-methylbenzamide (43): A white solid (39 mg, 37%); mp: 126.5–128 °C; ^{1}H NMR (270 MHz, $CDCl_3$): δ = 1.66–1.83 (m, 6H), 1.90 (d, *J* = 2.7 Hz, 6H), 2.07 (brs, 3H), 2.96 (d, *J* = 4.9 Hz, 3H), 4.88 (s, 2H), 6.08 (brs, 1H), 6.83 (d app, *J* = 8.9 Hz, 2H), 7.68 (d app, *J* = 9.1 Hz, 2H); LC–MS (APCI) *m/z*: 351 $[M+Na]^+$; HRMS (FAB) *m/z* $[M+H]^+$ calcd for $C_{20}H_{26}NO_3$: 329.1747, found: 329.1755; HPLC: t_R = 2.55 min (98%) in 10% H_2O/CH_3CN.

4-(2-Adamantan-1-yl-2-oxoethoxy)-*N*-ethylbenzamide (44): A white solid (60 mg, 55%); mp: 141–142.5 °C; ^{1}H NMR (270 MHz, $CDCl_3$): δ = 1.20 (t, *J* = 7.4 Hz, 3H), 1.64–1.82 (m, 6H), 1.90 (d, *J* = 2.7 Hz, 6H), 2.07 (brs, 3H), 3.38–3.50 (m, 2H), 4.88 (s, 2H), 6.11 (brs, 1H), 6.83 (d app, *J* = 8.9 Hz, 2H), 7.68 (d app, *J* = 8.9 Hz, 2H); LC–MS (APCI) *m/z*: 340 $[M-H]^-$; HRMS (FAB) *m/z* $[M+H]^+$ calcd for $C_{21}H_{28}NO_3$: 342.2064, found: 342.2063; HPLC: t_R = 1.88 min (97%) in 10% H_2O/CH_3CN at 1.0 mL min^{-1}.

4-(2-Adamantan-1-yl-2-oxoethoxy)-*N*-isopropylbenzamide (45): A white solid (57. mg, 50%); mp: 161–167 °C; ^{1}H NMR (270 MHz, $CDCl_3$): δ = 1.21 (d, *J* = 6.7 Hz, 6H), 1.64–1.85 (m, 6H), 1.90 (d, *J* = 2.7 Hz, 6H), 2.06 (brs, 3H), 4.16–4.30 (m, 1H), 4.87 (s, 2H), 5.87 (d, *J* = 7.4 Hz, 1H), 6.82 (d app, *J* = 8.9 Hz, 2H), 7.65 (d app, *J* = 8.9 Hz, 2H); LC–MS (APCI) *m/z*: 354 $[M-H]^-$; HRMS (FAB) *m/z* $[M+H]^+$ calcd for $C_{22}H_{30}NO_3$: 356.2220, found: 356.2213; HPLC: t_R = 1.95 min (98%) in 10% H_2O/CH_3CN.

4-(2-Adamantan-1-yl-2-oxoethoxy)-*N*-*tert*-butylbenzamide (46): A white solid (41 mg, 35%); mp: 179–181 °C; ^{1}H NMR (270 MHz, $CDCl_3$): δ = 1.41 (s, 9H), 1.65–1.82 (m, 6H), 1.90 (d, *J* = 2.7 Hz, 6H), 2.07 (brs, 3H), 4.87 (s, 2H), 5.84 (brs, 1H), 6.83 (d app, *J* = 8.9 Hz, 2H), 7.64 (d app, *J* = 8.9 Hz, 2H); LC–MS (APCI) *m/z*: 368 $[M-H]^-$; HRMS (FAB) *m/z* $[M+H]^+$ calcd for $C_{23}H_{32}NO_3$: 370.2377, found: 370.2376; HPLC: t_R = 2.29 min (98%) in 10% H_2O/CH_3CN.

4-(2-Adamantan-1-yl-2-oxoethoxy)-*N*,*N*-diethylbenzamide (47): A white solid (44 mg, 37%); mp: 103–104.5 °C; ^{1}H NMR (270 MHz, $CDCl_3$): δ = 1.15 (brs, 6H), 1.64–1.84 (m, 6H), 1.91 (d, *J* = 2.7 Hz, 6H), 2.07 (brs, 3H), 3.37 (brs, 4H), 4.86 (s, 2H), 6.83 (d app, *J* = 8.9 Hz, 2H), 7.30 (d app, *J* = 8.9 Hz, 2H); LC–MS (APCI) *m/z*: 392 $[M+Na]^+$; HRMS (FAB) *m/z* $[M+H]^+$ calcd for $C_{23}H_{32}NO_3$: 370.2377, found: 370.2370; HPLC: t_R = 2.26 min (97%) in 10% H_2O/CH_3CN.

4-(2-Adamantan-1-yl-2-oxoethoxy)-*N*-phenylbenzamide (48): A white solid (55 mg, 44%); mp: 183–185 °C; ^{1}H NMR (270 MHz, $CDCl_3$): δ = 1.65–1.90 (m, 6H), 1.93 (s app, 6H), 2.09 (brs, 3H), 4.93 (s, 2H), 6.91 (d app, *J* = 8.9 Hz, 2H), 7.13 (t, *J* = 7.2 Hz, 1H), 7.35 (t, *J* = 7.4 Hz, 2H), 7.60 (d, *J* = 8.6 Hz, 2H), 7.71 (brs, 1H), 7.80 (d app, *J* = 8.7 Hz, 2H); LC–MS (APCI) *m/z*: 388 $[M-H]^-$; HRMS (FAB) *m/z* $[M+H]^+$ calcd for $C_{25}H_{28}NO_3$: 390.2064, found: 390.2066; HPLC: t_R = 2.18 min (99%) in 10% H_2O/CH_3CN.

4-(2-Adamantan-1-yl-2-oxoethoxy)-*N*-benzylbenzamide (49): A yellow solid (30 mg, 40%); mp: 143–146 °C; ^{1}H NMR (270 MHz, $CDCl_3$): δ = 1.85–1.62 (m, 6H), 1.90 (d, J = 2.7 Hz, 6H), 2.03 (brs, 3H), 4.60 (d, J = 5.7 Hz, 2H), 4.88 (s, 2H), 6.35 (t, J = 5.2 Hz, 1H), 6.84 (d app, J = 8.9 Hz, 2H), 7.24–7.34 (m, 5H), 7.72 (d app, J = 8.9 Hz, 2H); LC–MS (APCI) m/z: 402 $[M-H]^-$; HRMS (FAB) m/z $[M+H]^+$ calcd for $C_{26}H_{30}NO_3$: 404.2220, found: 404.2224; HPLC: t_R = 2.11 min (> 99%) in 10% H_2O/CH_3CN.

4-(2-Adamantan-1-yl-2-oxoethoxy)-*N*-furan-2-ylmethylbenzamide (50): A white solid (70 mg, 56%); mp: 158–160 °C; ^{1}H NMR (270 MHz, $CDCl_3$): δ = 1.63–1.83 (m, 6H), 1.90 (d, J = 2.7 Hz, 6H), 2.06 (brs, 3H), 4.58 (d, J = 5.5 Hz, 2H), 4.87 (s, 2H), 6.27 (ddd, J = 15.0, 3.0, 2.0 Hz, 1H), 6.44 (t, J = 4.9 Hz, 1H), 6.83 (d app, J = 8.9 Hz, 2H), 7.34 (dd, J = 2.0, 1.0 Hz, 1H), 7.71 (d app, J = 8.9 Hz, 2H); LC–MS (APCI) m/z: 392 $[M-H]^-$; HRMS (FAB) m/z $[M+H]^+$ calcd for $C_{24}H_{28}NO_4$: 394.2013, found: 394.2016; HPLC: t_R = 1.89 min (96%) in 10% H_2O/CH_3CN.

3-(2-Adamantan-1-yl-2-oxoethoxy)benzamide (51): A white solid (24 mg, 18%); mp: 180.5–188 °C; ^{1}H NMR (270 MHz, $CDCl_3$): δ = 1.61–1.84 (m, 6H), 1.90 (d, J = 3.0 Hz, 6H), 2.06 (brs, 3H), 4.90 (s, 2H), 5.81 (brs, 1H), 6.18 (brs, 1H), 6.98–7.11 (m, 1H), 7.24–7.33 (m, 3H); LC–MS (APCI) m/z: 312 $[M-H]^-$; HRMS (FAB) m/z $[M+H]^+$ calcd for $C_{19}H_{24}NO_3$: 314.1751, found: 314.1758; HPLC: t_R = 2.05 min (98%) in 10% H_2O/CH_3CN.

3-(2-Adamantan-1-yl-2-oxoethoxy)-*N*-methylbenzamide (52): A white solid(63 mg, 61%); mp: 183.5–185.5 °C; ^{1}H NMR (270 MHz, $CDCl_3$): δ = 1.82–1.64 (m, 6H), 1.90 (d, J = 2.7 Hz, 6H), 2.06 (brs, 3H), 2.96 (d, J = 4.9 Hz, 3H), 4.88 (s, 2H), 6.32 (brs, 1H), 6.95–7.03 (m, 1H), 7.22–7.31 (m, 3H); LC–MS (APCI) m/z: 326 $[M-H]^-$; HRMS (FAB) m/z $[M+H]^+$ calcd for $C_{20}H_{26}NO_3$: 328.1907, found: 328.1893; HPLC: t_R = 2.12 min (97%) in 10% H_2O/CH_3CN.

3-(2-Adamantan-1-yl-2-oxoethoxy)-*N*-ethylbenzamide (53): Colourless crystals (57 mg, 52%); mp: 107–110 °C; ^{1}H NMR (270 MHz, $CDCl_3$): δ = 1.21 (t, J = 7.2 Hz, 3H), 1.63–1.82 (m, 6H), 1.89 (d, J = 2.7 Hz, 6H), 2.05 (brs, 3H), 3.38–3.50 (m, 2H), 4.87 (s, 2H), 6.27 (brs, 1H), 6.94–7.03 (m, 1H), 7.22–7.29 (m, 3H); LC–MS (APCI) m/z: 340 $[M-H]^-$; HRMS (FAB) m/z $[M+H]^+$ calcd for $C_{21}H_{28}NO_3$: 342.2064, found: 342.2051; HPLC: t_R = 2.50 min (98%) in 10% H_2O/CH_3CN.

3-(2-Adamantan-1-yl-2-oxoethoxy)-*N*-isopropylbenzamide (54): Colourless crystals (70 mg, 61%); mp: 158–161 °C; ^{1}H NMR (270 MHz, $CDCl_3$): δ = 1.21 (d, J = 6.4 Hz, 6H), 1.63–1.81 (m, 6H), 1.88 (d, J = 2.7 Hz, 6H), 2.05 (brs, 3H), 4.15–4.30 (m, 1H), 4.87 (s, 2H), 6.03 (d, J = 7.4 Hz, 1H), 6.93–7.02 (m, 1H), 7.22–7.29 (m, 3H); LC–MS (APCI) m/z: 354 $[M-H]^-$; HRMS (FAB) m/z $[M+H]^+$ calcd for $C_{22}H_{30}NO_3$: 356.2220, found: 356.2213; HPLC: t_R = 2.66 min (98%) in 10% H_2O/CH_3CN.

3-(2-Adamantan-1-yl-2-oxoethoxy)-*N*-*tert*-butylbenzamide (55): A white solid (67 mg, 57%); mp: 139.5–141 °C; ^{1}H NMR (270 MHz, $CDCl_3$): δ = 1.43 (s, 9H), 1.66–1.80 (m, 6H), 1.89 (d, J = 2.7 Hz, 6H), 2.06 (brs, 3H), 4.87 (s, 2H), 5.96 (brs, 1H), 6.90 (ddd, J = 7.7, 2.9, 1.7 Hz, 1H), 7.19–7.30 (m, 3H); LC–MS (APCI) m/z: 368 $[M-H]^-$; HRMS (FAB) m/z $[M+H]^+$ calcd for $C_{23}H_{32}NO_3$: 370.2377, found: 370.2364; HPLC: t_R = 2.82 min (> 99%) in 10% H_2O/CH_3CN.

3-(2-Adamantan-1-yl-2-oxoethoxy)-*N*-furan-2-ylmethylbenzamide (56): A white solid (110 mg, 88%); mp: 120.5–123.5 °C; ^{1}H NMR (270 MHz, $CDCl_3$): δ = 1.61–1.80 (m, 6H), 1.86 (d, J = 2.7 Hz, 6H), 2.03 (brs, 3H), 4.55 (d, J = 5.6 Hz, 2H), 4.84 (s, 2H), 6.22 (dd, J = 3.2, 1.0 Hz, 1H), 6.28 (dd, J = 3.2, 1.8 Hz, 1H), 6.77 (brt, J = 5.0 Hz, 1H), 6.97 (ddd, J = 7.9, 2.7, 1.2 Hz, 1H), 7.19–7.37 (m, 4H); LC–MS (APCI) m/z: 392 $[M-H]^-$; HRMS (FAB) m/z $[M+H]^+$ calcd for $C_{24}H_{28}NO_4$: 394.2013, found: 394.2006; HPLC: t_R = 2.28 min (> 99%) in 10% H_2O/CH_3CN.

3-(2-Adamantan-1-yl-2-oxoethoxy)-*N*-benzylbenzamide (57): A white solid (77 mg, 60%); mp: 135.5–139 °C; ^{1}H NMR (270 MHz, $CDCl_3$): δ = 1.64–1.82 (m, 6H), 1.88 (d, J = 2.7 Hz, 6H), 2.05 (brs, 3H), 4.59 (d, J = 5.7 Hz, 2H), 4.87 (s, 2H), 6.57 (brt, J = 5.2 Hz, 1H), 7.01 (dt, J = 7.0, 2.5 Hz, 1H), 7.22–7.34 (m, 8H); LC–MS (APCI) m/z: 402 $[M-H]^-$; HRMS (FAB) m/z $[M+H]^+$ calcd for $C_{26}H_{30}NO_3$: 404.2220, found: 404.2215; HPLC: t_R = 2.43 min (98%) in 10% H_2O/CH_3CN.

3-(2-Adamantan-1-yl-2-oxoethoxy)-*N*-phenylbenzamide (58): Colourless crystals (89 mg, 71%); mp: 148–151 °C; ^{1}H NMR (270 MHz, $CDCl_3$): δ = 1.64–1.82 (m, 6H), 1.90 (d, J = 2.7 Hz, 6H), 2.06 (brs, 3H), 4.87 (s, 2H), 7.00 (ddd, J = 8.0, 2.7, 1.2 Hz, 1H), 7.13 (tt, J = 7.4, 1.2 Hz, 1H), 7.26–7.40 (m, 5H), 7.63 (dt, J = 9.0 Hz, 2H), 8.12 (brs, 1H); LC–MS (APCI) m/z: 388 $[M-H]^-$; HRMS (FAB) m/z $[M+H]^+$ calcd for $C_{25}H_{28}NO_3$: 390.2064, found: 390.2058; HPLC: t_R = 3.10 min (99%) in 10% H_2O/CH_3CN.

[4-(2-Adamantan-1-yl-2-oxoethoxy)phenyl]acetic acid (59): Hydrolysis of **25** (965 mg, 2.82 mmol) in MeOH/H_2O (24–4 mL) with LiOH (355 mg, 8.45 mmol) at RT gave the target compound as a white solid (886 mg, 96%); mp: 152.2–153.6 °C; ^{1}H NMR (270 MHz, $CDCl_3$): δ = 1.65–1.82 (m, 6H), 1.90 (d, J = 2.7 Hz, 6H), 2.07 (brs, 3H), 3.56 (s, 2H), 4.82 (s, 2H), 6.81 (d, J = 8.9 Hz, 2H), 7.17 (d, J = 8.9 Hz, 2H); LC–MS (APCI) m/z: 327 $[M-H]^-$; HRMS (FAB) m/z $[M+H]^+$ calcd for $C_{20}H_{25}O_4$: 329.1747, found: 329.1748; HPLC: t_R = 1.23 min (97%) in 10% H_2O/CH_3CN.

4-(2-Adamantan-1-yl-2-oxoethoxymethyl)benzoic acid (60): Hydrolysis of **32** (294 mg, 0.86 mmol) in THF/H_2O (8–1 mL) with LiOH (105 mg, 2.57 mmol) at RT gave the target compound as a white solid (162 mg, 57%); mp: > 260 °C (dec.); ^{1}H NMR (270 MHz, $CDCl_3$): δ = 1.61–1.79 (m, 6H), 1.81 (d, J = 2.7 Hz, 6H), 2.02 (brs, 3H), 4.35 (s, 2H), 4.64 (s, 2H), 7.46 (d, J = 8.4 Hz, 2H), 8.07 (d, J = 8.4 Hz, 2H); LC–MS (APCI) m/z: 327 $[M-H]^-$; HRMS (FAB) m/z $[M+H]^+$ calcd for $C_{20}H_{25}O_4$ $[M+H]^+$ 329.1747, found: 329.1751; HPLC: t_R = 1.67 min (97%) in 10% H_2O/CH_3CN.

Method D: Synthesis of carboxamide derivatives 61–73

2-[4-(2-Adamantan-1-yl-2-oxoethoxy)phenyl]-*N*-methyl-acetamide (61): A cream solid (41 mg, 40%); mp: 161–162 °C; ^{1}H NMR (270 MHz, $CDCl_3$): δ = 1.65–1.83 (m, 6H), 1.90 (d, J = 2.7 Hz, 6H), 2.07 (brs, 3H), 2.72 (d, J = 4.7 Hz, 3H), 3.48 (s, 2H), 4.85 (s, 2H),5.39 (brs, 1H), 6.81 (d app, J = 8.6 Hz, 2H), 7.12 (d app, J = 8.9 Hz, 2H); LC–MS (APCI) m/z: 340 $[M-H]^-$; HRMS (FAB) m/z $[M+H]^+$ calcd for $C_{21}H_{28}NO_3$: 342.2064, found: 342.2052; HPLC: t_R = 2.21 min (97%) in 10% H_2O/CH_3CN.

2-[4-(2-Adamantan-1-yl-2-oxoethoxy)phenyl]-*N*,*N*-dimethyl-acetamide (62): A yellow oil (54 mg, 51%); ^{1}H NMR (270 MHz, $CDCl_3$): δ = 1.65–1.82 (m, 6H), 1.88 (d, J = 2.7 Hz, 6H), 2.09 (brs, 3H), 2.92 (s, 3H), 2.96 (s, 3H), 3.61 (s, 2H), 4.81 (s, 2H), 6.73–6.82 (m, 2H), 7.08–7.16 (m, 2H); LC–MS (APCI) m/z: 354 $[M-H]^-$; HRMS (FAB) m/z $[M+H]^+$ calcd for $C_{22}H_{30}NO_3$: 356.2220, found: 356.2230; HPLC: t_R = 2.38 min (99%) in 10% H_2O/CH_3CN.

2-[4-(2-Adamantan-1-yl-2-oxoethoxy)phenyl]acetamide (63): A cream solid (61 mg, 31%); mp: 101–106 °C; ^{1}H NMR (270 MHz, $CDCl_3$): δ = 1.60–1.85 (m, 6H), 1.90 (d, J = 2.7 Hz, 6H), 2.06 (brs, 3H), 3.48 (s, 2H), 4.84 (s, 2H), 5.46 (brs, 1H), 5.62 (brs, 1H), 6.70–6.86 (m, 2H), 7.08–7.20 (m, 2H); LC–MS (APCI) m/z: 326 $[M-H]^-$;

HRMS (FAB) *m/z* $[M+H]^+$ calcd for $C_{20}H_{26}NO_3$: 328.1907, found: 328.1912; HPLC: t_R = 1.92 min (> 99%) in 10% H_2O/CH_3CN.

2-[4-(2-Adamantan-1-yl-2-oxoethoxy)phenyl]-*N*-ethyl-acetamide (64): A cream solid (55 mg, 52%); mp: 141.5–146.5 °C; ^{1}H NMR (270 MHz, $CDCl_3$): δ = 1.03 (t, *J* = 7.2 Hz, 3H), 1.64–1.82 (m, 6H), 1.90 (d, *J* = 2.7 Hz, 6H), 2.06 (brs, 3H), 3.27 (m, 2H), 3.46 (s, 2H), 4.84 (s, 2H), 5.40 (brs, 1H), 6.81 (d app, *J* = 8.7 Hz, 2H), 7.12 (d app, *J* = 8.9 Hz, 2H); LC–MS (APCI) *m/z*: 354 $[M-H]^-$; HRMS (FAB) *m/z* $[M+H]^+$ calcd for $C_{22}H_{30}NO_3$: 356.2220, found: 356.2220; HPLC: t_R = 2.06 min (96%) in 10% H_2O/CH_3CN.

2-[4-(2-Adamantan-1-yl-2-oxoethoxy)phenyl]-*N*-isopropyl-acetamide (65): A cream solid (51 mg, 46%); mp: 132–135 °C; ^{1}H NMR (270 MHz, $CDCl_3$): δ = 1.03 (d, *J* = 6.4 Hz, 6H), 1.65–1.83 (m, 6H), 1.90 (d, *J* = 2.7 Hz, 6H), 2.06 (brs, 3H), 3.44 (s, 2H), 3.93–4.15 (m, 1H), 4.84 (s, 2H), 5.18 (brd, *J* = 5.9 Hz, 1H), 6.82 (d app, *J* = 8.9 Hz, 2H), 7.13 (d app, *J* = 8.7 Hz, 2H); LC–MS (APCI) *m/z*: 368 $[M-H]^-$; HRMS (FAB) *m/z* $[M+H]^+$ calcd for $C_{23}H_{32}NO_3$: 370.2877, found: 370.2366; HPLC: t_R = 2.22 min (97%) in 10% H_2O/CH_3CN.

2-[4-(2-Adamantan-1-yl-2-oxoethoxy)phenyl]-*N*-*tert*-butyl-acetamide (66): A white solid (83 mg, 48%); mp: 144–145.5 °C; ^{1}H NMR (270 MHz, $CDCl_3$): δ = 1.24 (s, 9H), 1.64–1.89 (m, 6H), 1.89 (d app, *J* = 2.7 Hz, 6H), 2.05 (brs, 3H), 3.38 (s, 2H), 4.82 (s, 2H), 5.21 (brs, 1H), 6.80 (d app, *J* = 8.6 Hz, 2H), 7.10 (d app, *J* = 8.6 Hz, 2H); LC–MS (APCI) *m/z*: 382 $[M-H]^-$; HRMS (FAB) *m/z* $[M+H]^+$ calcd for $C_{24}H_{34}NO_3$: 384.2533, found: 384.2520; HPLC: t_R = 2.14 min (98%) in 10% H_2O/CH_3CN.

2-[4-(2-Adamantan-1-yl-2-oxoethoxy)phenyl]-*N*-benzyl-acetamide (67): A cream solid (89 mg, 71%); mp: 130.5–132.5 °C; ^{1}H NMR (270 MHz, $CDCl_3$): δ = 1.64–1.82 (m, 6H), 1.89 (d, *J* = 2.7 Hz, 6H), 2.06 (brs, 3H), 3.51 (s, 2H), 4.36 (d, *J* = 6.0 Hz, 2H), 4.81 (s, 2H), 5.88 (brs, 1H), 5.90 (d app, *J* = 8.7 Hz, 2H), 7.10–7.78 (m, 4H), 7.20–7.31 (m, 3H); LC–MS (APCI) *m/z*: 416 $[M-H]^-$; HRMS (FAB) *m/z* $[M+H]^+$ calcd for $C_{27}H_{32}NO_3$: 418.2377, found: 418.2368; HPLC: t_R = 2.07 min (99%) in 10% H_2O/CH_3CN.

2-[4-(2-Adamantan-1-yl-2-oxoethoxy)phenyl]-*N*-phenyl-acetamide (68): A cream solid (56 mg, 46%); mp: 152.5–154.5 °C; ^{1}H NMR (270 MHz, $CDCl_3$): δ = 1.66–1.84 (m, 6H), 1.91 (d, *J* = 2.9 Hz, 6H), 2.07 (brs, 3H), 3.64 (s, 2H), 4.86 (s, 2H), 6.52 (d app, *J* = 8.7 Hz, 2H), 7.60 (tt, *J* = 7.2, 1.2 Hz, 1H), 7.15–7.30 (m, 4H), 7.37–7.43 (m, 2H); LC–MS (APCI) *m/z*: 402 $[M-H]^-$; HRMS (FAB) *m/z* $[M+H]^+$ calcd for $C_{26}H_{30}NO_3$: 404.2220, found: 404.2206; HPLC: t_R = 2.21 min (98%) in 10% H_2O/CH_3CN.

2-[4-(2-Adamantan-1-yl-2-oxoethoxy)phenyl]-*N*-furan-2-ylmethyl-acetamide (69): A yellow semisolid (35 mg, 28%); ^{1}H NMR (270 MHz, $CDCl_3$): δ = 1.65–1.83 (m, 6H), 1.90 (d, *J* = 2.7 Hz, 6H), 2.07 (brs, 3H), 3.50 (s, 2H), 4.36 (d, *J* = 5.7 Hz, 2H), 4.84 (s, 2H), 5.74 (brs, 1H), 6.10–6.13 (m, 1H), 6.26 (dd, *J* = 3.2, 1.7 Hz, 1H), 6.81 (d app, *J* = 8.9 Hz, 2H), 7.13 (d app, *J* = 8.9 Hz, 2H), 7.29 (dd, *J* = 2.0, 1.0 Hz, 1H); LC–MS (APCI) *m/z*: 406 $[M-H]^-$; HRMS (FAB) *m/z* $[M+H]^+$ calcd for $C_{25}H_{30}NO_4$: 408.2169, found: 408.2174; HPLC: t_R = 2.17 min (96%) in 10% H_2O/CH_3CN.

4-(2-Adamantan-1-yl-2-oxoethoxymethyl)benzamide (70): A white solid (20 mg, 25%); mp: 143–149 °C; ^{1}H NMR (270 MHz, $CDCl_3$): δ = 1.59–1.83 (m, 6H), 1.85 (d, *J* = 2.7 Hz, 6H), 2.02 (brs, 3H), 4.32 (s, 2H), 4.61 (s, 2H), 5.58 (brs, 1H), 6.05 (brs, 1H), 7.44 (d, *J* = 5.9 Hz, 2H), 7.70–7.82 (m, 2H); LC–MS (APCI) *m/z*: 326 $[M-H]^-$; HRMS (FAB) *m/z* $[M+H]^+$ calcd for $C_{20}H_{26}NO_3$: 328.1907, found: 328.1913; HPLC: t_R = 3.18 min (> 99%) in 30% H_2O/CH_3CN.

4-(2-Adamantan-1-yl-2-oxoethoxymethyl)-*N*-methylbenzamide (71): A cream solid (43 mg, 60%); mp: 133.5–139 °C; ^{1}H NMR (270 MHz, $CDCl_3$): δ = 1.60–1.78 (m, 6H), 1.79 (d, *J* = 2.7 Hz, 6H), 2.01 (brs, 3H), 2.98 (d, *J* = 5.0 Hz, 3H), 4.31 (s, 2H), 4.58 (s, 2H), 6.29 (brd, *J* = 3.7 Hz, NH), 7.39 (d app, *J* = 8.4 Hz, 2H), 7.72 (d app, *J* = 8.4 Hz, 2H); LC–MS (APCI) *m/z*: 340 $[M-H]^-$; HRMS (FAB) *m/z* $[M+H]^+$ calcd for $C_{21}H_{28}NO_3$: 342.2064, found: 342.2051; HPLC: t_R = 2.11 min (97%) in 10% H_2O/CH_3CN.

4-(2-Adamantan-1-yl-2-oxoethoxymethyl)-*N*,*N*-dimethylbenzamide (72): A white solid (57 mg, 54%); mp: 76–80 °C; ^{1}H NMR (270 MHz, $CDCl_3$): δ = 1.58–1.80 (m, 6H), 1.80 (d, *J* = 2.7 Hz, 6H), 2.00 (brs, 3H), 2.96 (brs, 3H), 3.09 (brs, 3H), 4.31 (s, 2H), 4.58 (s, 2H), 7.39 (s, 4H); LC–MS (APCI) *m/z*: 354 $[M-H]^-$; HRMS (FAB) *m/z* $[M+H]^+$ calcd for $C_{22}H_{30}NO_3$: 356.2220, found: 356.2210; HPLC: t_R = 2.35 min (98%) in 10% H_2O/CH_3CN.

4-(2-Adamantan-1-yl-2-oxoethoxymethyl)-*N*-benzylbenzamide (73): An off-white solid (55 mg, 55%); mp: 126–131 °C; ^{1}H NMR (270 MHz, $CDCl_3$): δ = 1.58–1.75 (m, 6H), 1.79 (d, *J* = 2.9 Hz, 6H), 2.02 (brs, 3H), 4.30 (s, 2H), 4.58 (s, 2H), 4.62 (d, *J* = 5.7 Hz, 2H), 6.51 (brt, *J* = 5.3 Hz, NH), 7.23–7.36 (m, 5H), 7.39 (d app, *J* = 8.0 Hz, 2H), 7.76 (d app, *J* = 8.0 Hz, 2H); LC–MS (APCI) *m/z*: 416 $[M-H]^-$; HRMS (FAB) *m/z* $[M+H]^+$ calcd for $C_{27}H_{32}NO_3$: 418.2377, found: 418.2373; HPLC: t_R = 2.65 min (99%) in 10% H_2O/CH_3CN.

Method E: Synthesis of adamantyl ethanone thioether derivatives 74–82

A solution of 1-adamantyl bromomethyl ketone (1 equiv) in CH_3CN (15 mL) was treated with the corresponding thiophenol or thioalcohol (1.1 equiv), followed by Et_3N (3 equiv). The mixture was stirred at RT overnight. 2-Chloro-tritylchloride resin (1.1 equiv, 1.6 mmol g^{-1}) was added and the mixture was stirred for 2 h, filtered and concentrated in vacuo to give the crude product. Purification using flash chromatography yielded the title compound (yield 27–99%).

***N*-[3-(2-Adamantan-1-yl-2-oxoethylsulfanyl)phenyl]acetamide (74)**: Purification using flash chromatography (EtOAc/CH_2Cl_2; gradient elution) gave the title product (300 mg, 44%) as a white solid; mp: 122–123.5 °C; ^{1}H NMR (270 MHz, $CDCl_3$): δ = 1.64–1.78 (m, 6H), 1.85 (d, *J* = 2.7 Hz, 6H), 2.03 (brs, 3H), 2.13 (s, 3H), 3.93 (s, 2H), 7.04 (d, *J* = 8.2 Hz, 1H), 7.18 (t, *J* = 8.2 Hz, 1H), 7.33 (d, *J* = 8.2 Hz, 1H), 7.45 (brs, 1H), 7.53 (brs, 1H); LC–MS (ESI) *m/z*: 342 $[M-H]^-$; HRMS (ESI) *m/z* $[M+Na]^+$ calcd for $C_{20}H_{25}NO_2SNa$: 366.1504, found: 366.1470; HPLC: t_R = 2.27 min (99%) in 10% H_2O/CH_3CN.

***N*-[4-(2-Adamantan-1-yl-2-oxoethylsulfanyl)phenyl]acetamide (75)**: Purification using flash chromatography (EtOAc/CH_2Cl_2; gradient elution) yielded the title compound as a white solid (520 mg, 78%); mp: 110–111 °C; ^{1}H NMR (270 MHz, $CDCl_3$): δ = 1.62–1.75 (m, 6H), 1.82 (d, *J* = 2.8 Hz, 6H), 2.03 (brs, 3H), 2.16 (s, 3H), 3.86 (s, 2H), 7.21 (brs, 1H), 7.34 (dd, *J* = 7.0, 2.0 Hz, 2H), 7.42 (dd, *J* = 7.0, 2.0 Hz, 2H); LC–MS (APCI) *m/z*: 342 $[M-H]^-$; HRMS (FAB) *m/z* $[M+Na]^+$ calcd for $C_{20}H_{25}NO_2SNa$: 366.1504, found: 366.1476; HPLC: t_R = 5.25 min (> 99%) in 10% H_2O/CH_3CN.

1-Adamantan-1-yl-2-(4-chloro-phenylsulfanyl)ethanone (76): Purification using flash chromatography (hexane/CH_2Cl_2; gradient elution) yielded the title compound as a white crystalline solid (98 mg, 61%); mp: 90–91 °C; ^{1}H NMR (270 MHz, $CDCl_3$): δ = 1.64–1.76 (m, 6H), 1.83 (d, *J* = 2.8 Hz, 6H), 2.04 (brs, 3H), 3.88 (s, 2H), 7.20–7.26 (m, 4H); LC–MS (APCI) *m/z*: 319 $[M-H]^-$; HRMS (FAB)

m/z $[M+Na]^+$ calcd for $C_{18}H_{21}ClOSNa$: 343.0899, found: 343.0895; HPLC: $t_R = 4.23$ min (> 98%) in 20% H_2O/CH_3CN.

1-Adamantan-1-yl-2-*p*-tolylsulfanyl-ethanone (77): Purification using flash chromatography (hexane/CH_2Cl_2; gradient elution) yielded the title compound as a white crystalline solid (107 mg, 71%); mp: 65–67.5 °C; ^{1}H NMR (270 MHz, $CDCl_3$): $\delta = 1.62$ (m, 6H), 1.77 (d, $J = 3.0$ Hz, 6H), 1.97 (brs, 3H), 2.23 (s, 3H), 3.80 (s, 2H), 7.02 (d, $J = 7.9$ Hz, 2H), 7.21 (d, $J = 7.9$ Hz, 2H); LC–MS (APCI) *m/z*: 299 $[M-H]^-$; HRMS (FAB) *m/z* $[M+Na]^+$ calcd for $C_{19}H_{24}OSNa$: 323.1446, found: 323.1422; HPLC: $t_R = 4.44$ min (> 99%) in 20% H_2O/CH_3CN.

1-Adamantan-1-yl-2-(4-chloro-benzylsulfanyl)ethanone (78): Purification using flash chromatography (hexane/EtOAc; gradient elution) yielded the title compound as a white crystalline solid (330 mg, 99%); mp: 73–75 °C; ^{1}H NMR (300 MHz, $CDCl_3$): $\delta = 1.66$–1.78 (m, 6H), 1.83 (d, $J = 2.8$ Hz, 6H), 2.06 (brs, 3H), 3.20 (s, 2H), 3.70 (s, 2H), 7.26 (s, 4H); LC–MS (APCI) *m/z*: 333 $[M-H]^-$; HRMS (FAB) *m/z* $[M+Na]^+$ calcd for $C_{19}H_{23}ClOSNa$: 357.1056, found: 357.1035; HPLC: $t_R = 3.55$ min (> 98%) in 4% H_2O/CH_3CN.

1-Adamantan-1-yl-2-(2-chloro-benzylsulfanyl)ethanone (79): Purification using flash chromatography (hexane/EtOAc; gradient elution) yielded the title compound as a white solid (123 mg, 95%); mp: 43–47 °C; ^{1}H NMR (270 MHz, $CDCl_3$): $\delta = 1.60$–1.80 (m, 6H), 7.57–7.52 (m, 1H), 1.83 (d, $J = 2.7$ Hz, 6H), 2.03 (brs, 3H), 3.29 (s, 2H), 3.83 (s, 2H), 7.14–7.23 (m, 2H), 7.32–7.39 (m, 2H); LC–MS (ESI) *m/z*: 357 $[M+Na]^+$; HRMS (FAB) *m/z* $[M+H]^+$ calcd for $C_{19}H_{24}ClOS$: 335.1231, found: 335.1225;HPLC: $t_R = 5.88$ min (98%) in 10% H_2O/CH_3CN.

1-Adamantan-1-yl-2-(3-methylbenzylsulfanyl)ethanone (80): Purification using flash chromatography (hexane/EtOAc; gradient elution) gave the title compound as a transparent oil (110 mg, 27%); ^{1}H NMR (270 MHz, $CDCl_3$): $\delta = 1.62$–1.78 (m, 6H), 1.81 (d, $J = 2.9$ Hz, 6H), 2.02 (brs, 3H), 2.32 (s, 3H), 3.22 (s, 2H), 3.68 (s, 2H), 7.03–7.21 (m, 4H); LC–MS (APCI) *m/z*: 337 $[M+Na]^+$; HRMS (FAB) *m/z* $[M+H]^+$ calcd for $C_{20}H_{27}OS$: 315.1777, found: 315.1790; HPLC: $t_R = 9.56$ min (97%) in 10% H_2O/CH_3CN.

1-Adamantan-1-yl-2-(4-*tert*-butylbenzylsulfanyl)ethanone (81): A white solid (132 mg, 95%); mp: 64.5–68 °C; ^{1}H NMR (270 MHz, $CDCl_3$): $\delta = 1.29$ (s, 9H), 1.54–1.79 (m, 6H), 1.80 (m, 6H), 2.01 (brs, 3H), 3.17 (s, 2H), 3.68 (s, 2H), 7.22–7.34 (m, 4H); LC–MS (APCI) *m/z*: 357 $[M+H]^+$; HRMS (FAB) *m/z* $[M+H]^+$ calcd for $C_{23}H_{33}OS$: 357.2247, found: 357.2248; HPLC: $t_R = 14.9$ min (100%) in 10% H_2O/CH_3CN.

1-Adamantan-1-yl-2-(2,4-dichloro-benzylsulfanyl)ethanone (82): A clear semisolid (127 mg, 88%); ^{1}H NMR (270 MHz, $CDCl_3$): $\delta =$ 1.62–1.78 (m, 6H) 1.83 (d, $J = 3.0$ Hz, 6H), 2.03 (brs, 3H), 3.26 (s, 2H), 3.79 (s, 2H), 7.19 (dd, $J = 8.0$, 2.0 Hz, 1H), 7.33 (d, $J = 8.0$ Hz, 1H), 7.38 (d, $J = 2.0$ Hz, 1H); LC–MS (APCI) *m/z*: 369 $[M+H]^+$; HRMS (FAB) *m/z* $[M+H]^+$ calcd for $C_{19}H_{23}Cl_2OS$: 369.0841 found 369.0847; HPLC: $t_R = 12.93$ min (> 99%) in 10% H_2O/CH_3CN.

***N*-[3-(2-Adamantan-1-yl-2-oxoethanesulfinyl)phenyl]acetamide (83) and *N*-[3-(2-adamantan-1-yl-2-oxoethanesulfonyl)phenyl]acetamide (91)**: A cold solution of **74** (270 mg, 0.79 mmol) in CH_2Cl_2 (30 mL) was treated with *m*-CPBA (215 mg, 60–77% purity). The mixture was stirred at −10 °C for 45 min, partitioned between CH_2Cl_2 and 5% aq Na_2CO_3. The organic phase was washed with brine, dried over $MgSO_4$ and concentrated in vacuo. Purification using flash chromatography (EtOAc/CH_2Cl_2; gradient elution) yielded **83** as a white solid (177 mg, 62%); mp: 73–76 °C; ^{1}H NMR (270 MHz, $CDCl_3$): $\delta = 1.59$–1.73 (m, 12H), 2.00 (brs, 3H), 2.21 (s, 3H), 3.78 (d, $J = 16$ Hz, 1H), 4.13 (d, $J = 16$ Hz, 1H), 7.20 (d, $J =$ 8.0 Hz, 1H), 7.42 (t, $J = 7.8$ Hz, 1H), 7.89 (s, 1H), 8.14 (d, $J = 8.0$ Hz, 1H), 8.68 (s, 1H); LC–MS (ESI) *m/z*: 358 $[M-H]^-$; HRMS (ESI) *m/z* $[M+Na]^+$ calcd for $C_{20}H_{25}NNaO_3S$: 382.1453, found: 382.1426; HPLC: $t_R = 1.71$ min (> 99%) in 10% H_2O/CH_3CN. Compound **91** was obtained as a white solid (21 mg, 7%); mp: 167–168 °C; ^{1}H NMR (270 MHz, $CDCl_3$): $\delta = 1.60$–1.75 (m, 12H), 2.03 (brs, 3H), 2.20 (s, 3H), 4.32 (s, 2H), 7.51 (t, $J = 8.1$ Hz, 1H), 7.64 (d, $J = 8.3$ Hz, 2H), 7.88 (s, 1H), 8.12 (d, $J = 8.2$ Hz, 1H); LC–MS (ESI) *m/z*: 374 $[M-H]^-$; HRMS (ESI) *m/z* $[M+Na]^+$ calcd for $C_{20}H_{25}NNaO_4S$: 398.1402, found: 398.1383; HPLC: $t_R = 1.74$ min (98%) in 10% H_2O/CH_3CN.

Method F: Synthesis of the adamantyl ethanone sulfoxide derivatives 84–90

A cold solution of the corresponding thioether derivative (1 equiv) in CH_2Cl_2 (10 mL) was treated with *m*-CPBA (1.2 equiv). The mixture was stirred at −10 °C for 20 min, partitioned between CH_2Cl_2 and 5% aq Na_2CO_3. The organic phase was washed with brine, dried over $MgSO_4$ and concentrated in vacuo to give crude product. Purification using flash chromatography (EtOAc/CH_2Cl_2; gradient elution) yielded the title compound (20–80%).

***N*-[4-(2-Adamantan-1-yl-2-oxoethanesulfinyl)phenyl]acetamide (84)**: Purification using flash chromatography (EtOAc/CH_2Cl_2; gradient elution) yielded the title compound as a white solid (200 mg, 76%); mp: 173.5–175.5 °C; ^{1}H NMR (270 MHz, $CDCl_3$): $\delta = 1.59$–1.73 (m, 12H), 2.01 (brs, 3H), 2.19 (s, 3H), 3.78 (d, $J = 5.6$ Hz, 1H), 4.15 (d, $J = 5.6$ Hz, 1H), 7.65 (m, 5H); LC–MS (APCI) *m/z*: 358 $[M-H]^-$; HRMS (FAB) *m/z* $[M+H]^+$ calcd for $C_{20}H_{26}NO_3S$: 360.1633, found: 360.1621; HPLC: $t_R = 4.35$ min (> 99%) in 10% H_2O/CH_3CN.

1-Adamantan-1-yl-2-(4-chloro-benzenesulfinyl)ethanone (85): A white solid (46 mg, 44%); mp: 144–146.5 °C; ^{1}H NMR (270 MHz, $CDCl_3$): $\delta = 1.55$–1.78 (m, 12H), 2.01 (brs, 3H), 3.80 (d, $J = 15.3$ Hz, 1H), 4.15 (d, $J = 15.3$ Hz, 1H), 7.49 (dt, $J = 8.9$, 2.2 Hz, 2H), 7.64 (dt, $J = 8.6$, 2.5 Hz, 2H); LC–MS (APCI) *m/z*: 335 $[M-H]^-$; HRMS (FAB) *m/z* $[M+H]^+$ calcd for $C_{18}H_{22}ClO_2S$: 337.1024, found: 337.1018; HPLC: $t_R = 5.74$ min (> 99%) in 10% H_2O/CH_3CN.

1-Adamantan-1-yl-2-(toluene-4-sulfinyl)ethanone (86): A white solid (70 mg, 67%); mp: 116.5–118 °C; ^{1}H NMR (270 MHz, $CDCl_3$): $\delta = 1.57$–1.74 (m, 12H), 1.99 (brs, 3H), 2.39 (s, 3H), 3.75 (d, $J =$ 15.1 Hz, 1H), 4.13 (d, $J = 15.3$ Hz, 1H), 7.30 (d app, $J = 7.9$ Hz, 2H), 7.56 (d app, $J = 8.1$ Hz, 2H); LC–MS (APCI) *m/z*: 315 $[M-H]^-$; HRMS (FAB) *m/z* $[M+H]^+$ calcd for $C_{19}H_{25}O_2S$: 317.1570, found: 317.1558; HPLC: $t_R = 5.42$ min (99%) in 10% H_2O/CH_3CN.

1-Adamantan-1-yl-2-(4-chloro-phenylmethanesulfinyl)ethanone (87): Purification using flash chromatography (EtOAc/CH_2Cl_2; gradient elution) yielded the title compound as a white crystalline solid (95 mg, 46%); mp: 164–166 °C; ^{1}H NMR (300 MHz, $CDCl_3$): $\delta = 1.65$–1.75 (m, 6H), 1.86 (brs, 6H), 2.10 (brs, 3H), 3.57 (d, $J = 15.6$ Hz, 1H), 3.90 (d, $J = 15.7$ Hz, 1H), 4.00 (d, $J = 13.2$ Hz, 1H), 4.11 (d, $J =$ 13.2 Hz, 1H), 7.25 (dt, $J = 8.3$, 2.0 Hz, 2H), 7.37 (dt, $J = 8.2$, 2.0 Hz, 2H); LC–MS (APCI) *m/z*: 351 $[M+H]^+$; HRMS (FAB) *m/z* $[M+H]^+$ calcd for $C_{19}H_{24}ClO_2S$: 351.1186, found: 351.1181; HPLC: $t_R =$ 3.09 min (> 99%) in 10% H_2O/CH_3CN.

1-Adamantan-1-yl-2-(2-chloro-phenylmethanesulfinyl)ethanone (88): The title compound was prepared as a white solid (190 mg, 80%); mp: 105.5–108 °C; ^{1}H NMR (270 MHz, $CDCl_3$): $\delta = 1.57$–1.85 (m, 12H), 2.03 (brs, 3H), 3.75 (d, $J = 15.5$ Hz, 1H), 3.92 (d, $J =$ 15.5 Hz, 1H), 4.15 (d, $J = 13.0$ Hz, 1H), 4.42 (d, $J = 13.0$ Hz, 1H),

7.22–7.30 (m, 2H), 7.36–7.44 (m, 2H); LC–MS (ESI) *m/z* 373 $[M+Na]^+$; HRMS (FAB) *m/z* $[M+H]^+$ calcd for $C_{19}H_{24}ClO_2S$: 351.1186, found: 351.1176; HPLC: $t_R = 2.54$ min (99%) in 10% H_2O/CH_3CN.

1-Adamantan-1-yl-2-(4-*tert*-butyl-phenylmethanesulfinyl)ethanone (89): A white solid (21 mg, 20%); mp: 144.5–146 °C; ^1H NMR (270 MHz, $CDCl_3$): $\delta = 1.27$ (s, 9H), 1.61–1.79 (m, 12H), 2.03 (m, 3H), 3.58 (d, $J = 15.6$ Hz, 1H), 3.86 (d, $J = 15.6$ Hz, 1H), 4.05 (d, $J = 13.0$ Hz, 1H), 4.20 (d, $J = 13.0$ Hz, 1H), 7.21 (d, $J = 8.4$ Hz, 2H), 7.37 (d, $J = 8.2$ Hz, 2H); LC–MS (APCI) *m/z*: 373 $[M+H]^+$; HRMS (FAB) *m/z* $[M+H]^+$ calcd for $C_{23}H_{33}O_2S$: 373.2196, found: 373.2194; HPLC: $t_R = 7.13$ min (>99%) in 10% H_2O/CH_3CN.

1-Adamantan-1-yl-2-(2,4-dichloro-benzylsulfanyl)ethanone (90): A white solid (56 mg, 56%); mp: 126–128 °C; ^1H NMR (270 MHz, $CDCl_3$): $\delta = 1.64$–1.85 (m, 12H), 2.07 (m, 3H), 3.78 (d, $J = 15.6$ Hz, 1H), 3.95 (d, $J = 15.6$ Hz, 1H), 4.12 (d, $J = 13.1$ Hz, 1H), 4.42 (d, $J = 12.9$ Hz, 1H), 7.28 (d, $J = 2.0$ Hz, 1H), 7.36 (d, $J = 8.4$ Hz, 1H), 7.46 (d, $J = 2.0$ Hz, 1H); LC–MS (APCI) *m/z*: 385 $(M+1)^+$; HRMS (FAB) *m/z* $[M+H]^+$ calcd for $C_{19}H_{23}Cl_2O_2S$: 385.0790, found: 385.0788; HPLC: $t_R = 6.19$ min (>99%) in 10% H_2O/CH_3CN.

Method G: Synthesis of adamantyl ethanone sulfone derivatives 92–99

A solution of the corresponding sulfoxide derivative (1 equiv) in CH_2Cl_2 (10 mL) was treated with *m*-CPBA (2 equiv). The mixture was stirred at RT and monitored by TLC. After completion, the mixture was partitioned between CH_2Cl_2 and 5% aq Na_2CO_3. The organic phase was washed with brine, dried over $MgSO_4$ and concentrated in vacuo to give crude product. Purification using flash chromatography (EtOAc/CH_2Cl_2; gradient elution) yielded the title compound (29–99%).

***N*-[4-(2-Adamantan-1-yl-2-oxoethanesulfonyl)phenyl]acetamide (92)**: Purification using flash chromatography (EtOAc/CH_2Cl_2; gradient elution) yielded the title compound as a white solid (79 mg, 81%); mp: 151–151.5 °C; ^1H NMR (270 MHz, $CDCl_3$): $\delta = 1.56$–1.70 (m, 6H), 1.73 (d, $J = 2.7$ Hz, 6H), 2.04 (brs, 3H), 2.22 (s, 3H), 4.27 (s, 2H), 7.43 (brs, 1H), 7.69 (dt, $J = 8.7$, 2.2 Hz, 2H), 7.86 (dt, $J = 8.7$, 2.2 Hz, 2H); LC–MS (APCI) *m/z*: 374 $[M-H]^-$; HRMS (FAB) *m/z* $[M+Na]^+$ calcd for $C_{20}H_{25}NO_4SNa$: 398.1402, found: 398.1396; HPLC: $t_R = 1.85$ min (>99%) in 10% H_2O/CH_3CN.

1-Adamantan-1-yl-2-(4-chloro-benzenesulfonyl)ethanone (93): Purification using flash chromatography (hexane/EtOAc; gradient elution) yielded the title compound as a white crystalline solid (52 mg, 64%); mp: 165–166 °C; ^1H NMR (270 MHz, $CDCl_3$): $\delta = 1.69$ (m, 6H), 1.75 (d, $J = 2.8$ Hz, 6H), 2.05 (brs, 3H), 4.28 (s, 2H), 7.53 (dt, $J = 7.6$, 2.3 Hz, 2H), 7.88 (dt, $J = 7.5$, 2.1 Hz, 2H); LC–MS (APCI) *m/z*: 353 $[M+H]^+$; HRMS (FAB) *m/z* $[M+H]^+$ calcd for $C_{18}H_{22}ClO_3S$: 353.0978, found: 353.0969; HPLC: $t_R = 3.42$ min (>99%) in 20% H_2O/CH_3CN.

1-Adamantan-1-yl-2-(toluene-4-sulfonyl)ethanone (94): Purification using flash chromatography (hexane/EtOAc; gradient elution) yielded the title compound as a white crystalline solid (60 mg, 82%); mp: 146–147.5 °C; ^1H NMR (270 MHz, $CDCl_3$): $\delta = 1.53$–1.74 (m, 12H), 2.04 (brs, 3H), 2.44 (s, 3H), 4.26 (s, 2H), 7.53 (d, $J = 8.5$ Hz, 2H), 7.80 (d, $J = 8.5$ Hz, 2H); LC–MS (APCI) *m/z*: 331 $[M-H]^-$; HRMS (FAB) *m/z* $[M+Na]^+$ calcd for $C_{19}H_{24}O_3SNa$: 355.1344, found: 355.1344; HPLC: $t_R = 2.99$ min (>99%) in 10% H_2O/CH_3CN.

1-Adamantan-1-yl-2-(4-chloro-phenylmethanesulfonyl)ethanone (95): A white solid (40 mg, 68%); mp: 166.5–167.5 °C; ^1H NMR (270 MHz, $CDCl_3$): $\delta = 1.58$–1.68 (m, 6H), 1.73 (d, $J = 2.8$ Hz, 6H), 2.02 (brs, 3H), 3.80 (s, 2H), 4.40 (s, 2H), 7.30 (dt, $J = 8.2$, 2.0 Hz, 2H), 7.36 (dt, $J = 8.2$, 2.0 Hz, 2H); LC–MS (APCI) *m/z*: 367 $[M+H]^+$; HRMS (FAB) *m/z* $[M+NH_4]^+$ calcd for $C_{19}H_{27}ClNO_3S$: 384.1400, found: 384.1399; HPLC: $t_R = 3.14$ min (98%) in 10% H_2O/CH_3CN.

1-Adamantan-1-yl-2-(2-chloro-phenylmethanesulfonyl)ethanone (96): A white solid (270 mg, 94%); mp: 114–116.5 °C; ^1H NMR (270 MHz, $CDCl_3$): $\delta = 1.60$–1.82 (m, 6H), 1.82 (d, $J = 2.7$ Hz, 6H), 2.08 (brs, 3H), 4.08 (s, 2H), 4.77 (s, 2H), 7.26–7.36 (m, 2H), 7.42–7.47 (m, 1H), 7.52–7.57 (m, 1H); LC–MS (ESI): *m/z*: 365 $[M-H]^-$; HRMS (FAB) *m/z* $[M+H]^+$ calcd for $C_{19}H_{24}ClO_3S$: 367.1129, found: 367.1125; HPLC: $t_R = 2.72$ min (97%) 10% H_2O/CH_3CN.

1-Adamantan-1-yl-2-*m*-tolylmethanesulfonyl-ethanone (97): A white solid (277 mg, 81%); mp: 133–133.5 °C; ^1H NMR (270 MHz, $CDCl_3$): $\delta = 1.60$–1.75 (m, 6H), 1.77 (d, $J = 2.7$ Hz, 6H), 2.06 (brs, 3H), 2.34 (s, 3H), 3.88 (s, 2H), 4.47 (s, 2H), 7.13–7.31 (m, 4H); LC–MS (APCI) *m/z*: 345 $[M-H]^-$; HRMS (FAB) *m/z* $[M+H]^+$ calcd for $C_{20}H_{27}O_3S$: 347.1675, found: 347.1667; HPLC: $t_R = 2.21$ min (98%) in 10% H_2O/CH_3CN.

1-Adamantan-1-yl-2-(4-*tert*-butyl-phenylmethanesulfonyl)ethanone (98): A white solid (262 mg, 57%); mp: 173–174.5 °C; ^1H NMR (270 MHz, $CDCl_3$): $\delta = 1.30$ (s, 9H), 1.60–1.75 (m, 6H), 1.77 (d, $J = 2.9$ Hz, 6H), 2.08 (brs, 3H), 3.88 (s, 2H), 4.48 (s, 2H), 7.38 (s app, 4H); LC–MS (APCI) *m/z*: 387 $[M-H]^-$; HRMS (FAB) *m/z* $[M+H]^+$ calcd for $C_{23}H_{33}O_3S$: 389.2145, found: 389.2162; HPLC: $t_R = 3.10$ min (99%) in 10% H_2O/CH_3CN.

1-Adamantan-1-yl-2-(2,4-dichloro-phenylmethanesulfonyl)ethanone (99): A white solid (18 mg, 29%); mp: 171–173 °C; ^1H NMR (270 MHz, $CDCl_3$): $\delta = 1.60$–1.79 (m, 6H), 1.81 (d, $J = 2.7$ Hz, 6H), 2.08 (brs, 3H), 4.08 (s, 2H), 4.77 (s, 2H), 7.28 (dd, $J = 8.1$, 2.2 Hz, 1H), 7.47 (d, $J = 2.2$ Hz, 1H), 7.49 (d, $J = 8.4$ Hz, 1H); LC–MS (APCI) *m/z*: 399 $[M-H]^-$; HRMS (ESI) *m/z* $[M+H]^+$ calcd for $C_{19}H_{22}Cl_2O_3S$: 401.0739, found: 401.0745; HPLC: $t_R = 6.75$ min (98%) in 10% H_2O/MeOH.

3-(2-Adamantan-1-yl-2-oxoethylsulfanyl)benzoic acid (100): A solution of 1-adamantyl bromomethyl ketone (514 mg, 2.0 mmol) in CH_3CN (20 mL) was treated with 3-mercaptobenzoic acid (340 mg, 2.1 mmol) followed by Et_3N (2 mL). The mixture was stirred at RT overnight, partitioned between CH_2Cl_2 and brine. The organic phase was washed with brine, dried over $MgSO_4$ and concentrated in vacuo. Purification using flash chromatography gave the title compound as a white solid (550 mg, 83%); mp: 129–131 °C; ^1H NMR (270 MHz, $CDCl_3$): $\delta = 1.65$–1.80 (m, 6H), 1.87 (d, $J = 2.7$ Hz, 6H), 2.06 (brs, 3H), 4.00 (s, 2H), 7.38 (t, $J = 7.7$ Hz, 1H), 7.58 (dd, $J = 7.7$, 1.7 Hz, 1H), 7.91 (dd, $J = 7.7$, 1.7 Hz, 1H), 8.01 (d, $J = 1.7$ Hz, 1H); LC–MS (ESI) *m/z*: 329 $[M-H]^-$; HRMS (ESI) *m/z* $[M+Na]^+$ calcd for $C_{19}H_{22}O_3SNa$: 353.1187, found: 353.1159; HPLC: $t_R = 1.12$ min (98%) in 10% H_2O/CH_3CN.

3-{[2-(Adamantan-1-yl)-2-oxoethyl]sulfanyl}-*N*-methylbenzamide (101) The compound was prepared using method D. A white solid (70 mg, 68% yield) was obtained; mp: 122–123 °C; ^1H NMR (270 MHz, $CDCl_3$): $\delta = 1.62$–1.73 (m, 6H), 1.84 (d, $J = 2.7$ Hz, 6H), 2.04 (brs, 3H), 3.00 (d, $J = 4.4$ Hz, 3H), 3.96 (s, 2H), 6.14 (brs, 1H), 7.30 (d, $J = 7.7$ Hz, 2H), 7.43 (d, $J = 7.8$ Hz, 2H), 7.52 (d, $J = 7.7$ Hz, 2H) and 7.72 (s, 1H); LC–MS (APCI) *m/z*: 342 $[M-H]^-$; HRMS (ESI) *m/z* $[M+H]^+$ calcd for $C_{20}H_{26}NO_2S$: 344.1684, found: 344.1679; HPLC: $t_R = 2.2$ min (97%) in 10% H_2O/CH_3CN.

3-{[2-(Adamantan-1-yl)-2-oxoethyl]sulfanyl}-*N*,*N*-dimethyl benzamide (102): The compound was prepared using method D. A clear oil (190 mg, 65% yield) was obtained; ^1H NMR (270 MHz, $CDCl_3$):

δ = 1.65–1.76 (m, 6H), 1.83 (d, J = 2.7 Hz, 6H), 2.03 (br s, 3H), 2.96 (s, 3H), 3.09 (s, 3H), 3.95 (s, 2H), 7.19–7.39 (s, 1H); LC–MS (APCI) m/z: 356 $[M-H]^-$; HRMS (ESI) m/z $[M+H]^+$ calcd for $C_{21}H_{28}NO_2S$: 358.1841, found: 358.1819; HPLC: t_R = 2.2 min (97%) 10% H_2O/CH_3CN.

3-(2-Adamantan-1-yl-2-oxoethanesulfinyl)-*N*,*N*-dimethylbenzamide (103) and 3-(2-adamantan-1-yl-2-oxoethanesulfonyl)-*N*,*N*-dimethylbenzamide (104): A cold solution of **102** (177 mg, 0.33 mmol) in CH_2Cl_2 (15 mL) was treated with *m*-CPBA (96 mg, 60–77% purity). The mixture was stirred at −10 °C for 1.5 h, partitioned between CH_2Cl_2 and 5% aq Na_2CO_3. The organic phase was washed with brine, dried over $MgSO_4$ and concentrated in vacuo. Purification using flash chromatography (EtOAc/CH_2Cl_2; gradient elution) gave **103** as a clear oil (30 mg, 24%); ^{1}H NMR (270 MHz, $CDCl_3$): δ = 1.65–1.80 (m, 12H), 2.02 (br s, 3H), 2.95 (s, 3H), 3.10 (s, 3H), 3.76 (d, J = 15 Hz, 1H), 4.16 (d, J = 15 Hz, 1H), 7.55 (d, J = 4.9 Hz, 2H), 7.68–7.75 (m, 2H); LC–MS (ESI) m/z: 374 $[M+H]^+$; HRMS (ESI) m/z $[M+H]^+$ calcd for $C_{21}H_{28}NO_3S$: 374.1790, found: 374.1776; HPLC: t_R = 1.81 min (>99%) in 10% H_2O/CH_3CN. Compound **104** was obtained as a clear oil (90 mg, 70%); ^{1}H NMR (270 MHz, $CDCl_3$): δ = 1.58–1.72 (m, 12H), 2.03 (br s, 3H), 2.98 (s, 3H), 3.11 (s, 3H), 4.28 (s, 2H), 7.60 (t, J = 7.7 Hz, 1H), 7.72 (d, J = 7.7 Hz, 1H), 7.96–8.00 (m, 2H); LC–MS (ESI) m/z: 388 $[M-H]^-$; HRMS (ESI) m/z $[M+H]^+$ calcd for $C_{21}H_{28}NO_4S$: 390.1739, found: 390.1726; HPLC: t_R = 1.90 min (99%) in 10% H_2O/CH_3CN.

Acknowledgements

This work was supported by Sterix Ltd., a member of the Ipsen Group. We thank Ms. A. C. Smith for technical assistance, Dr. N. Muller and Dr. I. Viossat for the CYP inhibition and metabolic stability studies. We also thank the ESPRC national mass spectrometry service centre at the University of Wales (Swansea, UK) for some high-resolution accurate mass measurements.

Keywords: 11β-HSD1 · adamantyl ethanones · diabetes · hydroxysteroid dehydrogenase · inhibitors · metabolic syndrome

[1] S. M. Grundy, *J. Clin. Endocrinol. Metab.* **2004**, *89*, 2595 – 2600.
[2] T. C. Sandeep, B. R. Walker, *Trends Endocrinol. Metab.* **2001**, *12*, 446 – 453.
[3] J. W. Tomlinson, E. A. Walker, I. J. Bujalska, N. Draper, G. G. Lavery, M. S. Cooper, M. Hewison, P. M. Stewart, *Endocr. Rev.* **2004**, *25*, 831 – 866.
[4] B. R. Walker, *Diabetic Med.* **2006**, *23*, 1281 – 1288.
[5] R. Thieringer, A. Hermanowski-Vosatka, *Expert Rev. Cardiovasc. Ther.* **2005**, *3*, 911 – 924.
[6] J. E. Friedman, J. S. Yun, Y. M. Patel, M. M. McGrane, R. W. Hanson, *J. Biol. Chem.* **1993**, *268*, 12952 – 12957.
[7] M. Wang, *Nutr. Metab. (Lond.)* **2005**, *2*, 3.
[8] P. O. Hasselgren, *Curr. Opin. Clin. Nutr. Metab. Care* **1999**, *2*, 201 – 205.
[9] G. Arnaldi, A. Angeli, A. B. Atkinson, X. Bertagna, F. Cavagnini, G. P. Chrousos, G. A. Fava, J. W. Findling, R. C. Gaillard, A. B. Grossman, B. Kola, A. Lacroix, T. Mancini, F. Mantero, J. Newell-Price, L. K. Nieman, N. Sonino, M. L. Vance, A. Giustina, M. Boscaro, *J. Clin. Endocrinol. Metab.* **2003**, *88*, 5593 – 5602.
[10] B. S. McEwen, *J. Clin. Endocrinol. Metab.* **2002**, *87*, 1947 – 1948.
[11] A. Faggiano, R. Pivonello, S. Spiezia, M. C. De Martino, M. Filippella, C. Di Somma, G. Lombardi, A. Colao, *J. Clin. Endocrinol. Metab.* **2003**, *88*, 2527 – 2533.
[12] J. W. Chu, D. F. Matthias, J. Belanoff, A. Schatzberg, A. R. Hoffman, D. Feldman, *J. Clin. Endocrinol. Metab.* **2001**, *86*, 3568 – 3573.
[13] M. Wamil, J. R. Seckl, *Drug Discovery Today* **2007**, *12*, 504 – 520.
[14] R. Fraser, M. C. Ingram, N. H. Anderson, C. Morrison, E. Davies, J. M. C. Connell, *Hypertension* **1999**, *33*, 1364 – 1368.
[15] P. M. Stewart, C. B. Whorwood, *Steroids* **1994**, *59*, 90 – 95.
[16] U. C. T. Oppermann, B. Persson, H. Jörnvall, *Eur. J. Biochem.* **1997**, *249*, 355 – 360.
[17] J. R. Seckl, B. R. Walker, *Endocrinology* **2001**, *142*, 1371 – 1376.
[18] P. M. Stewart, A. M. Wallace, R. Valentino, D. Burt, C. H. L. Shackleton, C. R. W. Edwards, *Lancet* **1987**, *2*, 821 – 824.
[19] A. K. Agarwal, T. Mune, C. Monder, P. C. White, *J. Biol. Chem.* **1994**, *269*, 25959 – 25962.
[20] E. Rask, T. Olsson, S. Söderberg, R. Andrew, D. E. Livingstone, O. Johnson, B. R. Walker, *J. Clin. Endocrinol. Metab.* **2001**, *86*, 1418 – 1421.
[21] K. Kannisto, K. H. Pietiläinen, E. Ehrenborg, A. Rissanen, J. Kaprio, A. Hamsten, H. Yki-Järvinen, *J. Clin. Endocrinol. Metab.* **2004**, *89*, 4414 – 4421.
[22] H. Masuzaki, J. Paterson, H. Shinyama, N. M. Morton, J. J. Mullins, J. R. Seckl, J. S. Flier, *Science* **2001**, *294*, 2166 – 2170.
[23] E. E. Kershaw, N. M. Morton, H. Dhillon, L. Ramage, J. R. Seckl, J. S. Flier, *Diabetes* **2005**, *54*, 1023 – 1031.
[24] Y. Kotelevtsev, M. C. Holmes, A. Burchell, P. M. Houston, D. Schmoll, P. Jamieson, R. Best, R. Brown, C. R. W. Edwards, J. R. Seckl, J. J. Mullins, *Proc. Natl. Acad. Sci. USA* **1997**, *94*, 14924 – 14929.
[25] N. M. Morton, J. M. Paterson, H. Masuzaki, M. C. Holmes, B. Staels, C. Fievet, B. R. Walker, J. S. Flier, J. J. Mullins, J. R. Seckl, *Diabetes* **2004**, *53*, 931 – 938.
[26] P. Alberts, L. Engblom, N. Edling, M. Forsgren, G. Klingström, C. Larsson, Y. Rönquist-Nii, B. Ohman, L. Abrahmsén, *Diabetologia* **2002**, *45*, 1528 – 1532.
[27] P. Alberts, C. Nilsson, G. Selen, L. O. M. Engblom, N. H. M. Edling, S. Norling, G. Klingström, C. Larsson, M. Forsgren, M. Ashkzari, C. E. Nilsson, M. Fiedler, E. Bergqvist, B. Ohman, E. Björkstrand, L. B. Abrahmsén, *Endocrinology* **2003**, *144*, 4755 – 4762.
[28] A. Hermanowski-Vosatka, J. M. Balkovec, K. Cheng, H. Y. Chen, M. Hernandez, G. C. Koo, C. B. Le Grand, Z. H. Li, J. M. Metzger, S. S. Mundt, H. Noonan, C. N. Nunes, S. H. Olson, B. Pikounis, N. Ren, N. Robertson, J. M. Schaeffer, K. Shah, M. S. Springer, A. M. Strack, M. Strowski, K. Wu, T. J. Wu, J. Y. Xiao, B. B. Zhang, S. D. Wright, R. Thieringer, *J. Exp. Med.* **2005**, *202*, 517 – 527.
[29] B. R. Walker, A. A. Connacher, R. M. Lindsay, D. J. Webb, C. R. W. Edwards, *J. Clin. Endocrinol. Metab.* **1995**, *80*, 3155 – 3159.
[30] R. C. Andrews, O. Rooyackers, B. R. Walker, *J. Clin. Endocrinol. Metab.* **2003**, *88*, 285 – 291.
[31] M. Hawkins, D. Hunter, P. Kishore, S. Schwartz, M. Hompesch, G. Hollis, R. Levy, B. Williams, R. Huber, *Diabetes* **2008**, *57*, A99 – A100.
[32] J. W. Tomlinson, P. M. Stewart, *Nat. Clin. Pract. Endocrinol. Metab.* **2005**, *1*, 92 – 99.
[33] U. Oppermann, *Endocr. Metab. Immune Disord. Drug Targets* **2006**, 6, 259 – 269.
[34] S. P. Webster, T. D. Pallin, *Expert Opin. Ther. Pat.* **2007**, *17*, 1407 – 1422.
[35] K. A. Hughes, S. P. Webster, B. R. Walker, *Expert Opin. Invest. Drugs* **2008**, *17*, 481 – 496.
[36] X. Su, N. Vicker, B. V. L. Potter, *Prog. Med. Chem.* **2008**, *46*, 29 – 130.
[37] C. G. Schnackenberg, *Curr. Opin. Invest. Drugs* **2008**, *9*, 295 – 300.
[38] C. Fotsch, M. H. Wang, *J. Med. Chem.* **2008**, *51*, 4851 – 4857.
[39] C. Hale, M. Wang, *Mini-Rev. Med. Chem.* **2008**, *8*, 702 – 710.
[40] C. D. Boyle, *Curr. Opin. Drug Discov. Devel.* **2008**, *11*, 495 – 511.
[41] T. Barf, J. Vallgårda, R. Emond, C. Häggström, G. Kurz, A. Nygren, V. Larwood, E. Mosialou, K. Axelsson, R. Olsson, L. Engblom, N. Edling, Y. Rönquist-Nii, B. Ohman, P. Alberts, L. Abrahmsén, *J. Med. Chem.* **2002**, *45*, 3813 – 3815.
[42] B. G. Bhat, N. Hosea, A. Fanjul, J. Herrera, J. Chapman, F. Thalacker, P. M. Stewart, P. A. Rejto, *J. Pharmacol. Exp. Ther.* **2007**, *324*, 299 – 305.
[43] B. Sorensen, M. Winn, J. Rohde, Q. Shuai, J. Wang, S. Fung, K. Monzon, W. Chiou, D. Stolarik, H. Imade, L. Pan, X. Deng, L. Chovan, K. Longenecker, R. Judge, W. Qin, M. Brune, H. Camp, E. U. Frevert, P. Jacobson, J. T. Link, *Bioorg. Med. Chem. Lett.* **2007**, *17*, 527 – 532.
[44] C. Fotsch, M. D. Bartberger, E. A. Bercot, M. Chen, R. Cupples, M. Emery, J. Fretland, A. Guram, C. Hale, N. H. Han, D. Hickman, R. W. Hungate, M. Hayashi, R. Konlorowski, Q. Y. Liu, G. Matsumoto, D. J. S. Jean, S. Ursu, M. Veniant, G. F. Xu, Q. P. Ye, C. Yuan, J. D. Zhang, X. P. Zhang, H. Tu, M. H. Wang, *J. Med. Chem.* **2008**, *51*, 7953 – 7967.

[45] M. Henriksson, E. Homan, L. Johansson, J. Vallgårda, M. Williams, E. Bercot, C. H. Fotsch, A. Li, G. Cai, R. W. Hungate, C. C. Yuan, C. Tegley, D. St. Jean, N. Han, Q. Huang, Q. Liu, M. D. Bartberger, G. A. Moniz, M. J. Frizzle (Amgen Inc., USA; Biovitrum AB), PCT Application: WO2005116002, **2005**, p. 306.
[46] C. Fotsch, J. Adams, M. Bartberger, E. A. Bercot, L. Cai, V. M. Castro, M. Chen, R. Cupples, M. Emery, J. Fretland, A. Guram, S. Gustafsson, A. Hague, C. Hale, N. Han, M. Hayashi, M. Henriksson, D. Hickman, E. Homan, R. W. Hungate, L. Johansson, S. Jordan, C. Kaiser, R. Komorowski, A. Li, Q. Liu, G. Matsumoto, K. McRae, G. Moniz, G. Palm, D. Pyring, D. J. St. Jean, Jr., Y. Sun, M. Sydow-Backman, L. Tedenborg, H. Tu, S. Ursa, M. Veniant, M. Williams, G. Xu, Q. Ye, C. Yuan, J. Zhang, X. Zhang, M. Wang, *Abstracts of Papers*, *237th ACS National Meeting*, *Salt Lake City, UT (USA)*, *March 22 – 26*, *2009*, MEDI-029.
[47] N. Vicker, X. D. Su, D. Ganeshapillai, A. Smith, A. Purohit, M. J. Reed, B. V. L. Potter, *J. Steroid Biochem. Mol. Biol.* **2007**, *104*, 123 – 129.
[48] X. D. Su, N. Vicker, D. Ganeshapillai, A. Smith, A. Purohit, M. J. Reed, B. V. L. Potter, *Mol. Cell. Endocrinol.* **2006**, *248*, 214 – 217.
[49] D. J. Hosfield, Y. Q. Wu, R. J. Skene, M. Hilgers, A. Jennings, G. P. Snell, K. Aertgeerts, *J. Biol. Chem.* **2004**, *280*, 4639 – 4648.
[50] J. R. Patel, Q. Shuai, J. Dinges, M. Winn, M. Pliushchev, S. Fung, K. Monzon, W. Chiou, J. H. Wang, L. P. Pan, S. Wagaw, K. Engstrom, F. A. Kerdesky, K. Longenecker, R. Judge, W. Y. Qin, H. M. Imade, D. Stolarik, D. W. A. Beno, M. Brune, L. E. Chovan, H. L. Sham, P. Jacobson, J. T. Link, *Bioorg. Med. Chem. Lett.* **2007**, *17*, 750 – 755.
[51] C. Yuan, D. J. Jean, Q. Y. Liu, L. Cai, A. W. Li, N. H. Han, G. Moniz, B. Askew, R. W. Hungate, L. Johansson, L. Tedenborg, D. Pyring, M. Williams, C. Hale, M. Chen, R. Cupples, J. D. Zhang, S. Jordan, M. D. Bartberger, Y. X. Sun, M. Emery, M. H. Wang, C. Fotsch, *Bioorg. Med. Chem. Lett.* **2007**, *17*, 6056 – 6061.
[52] L. Johansson, C. Fotsch, M. D. Bartberger, V. M. Castro, M. Chen, M. Emery, S. Gustafsson, C. Hale, D. Hickman, E. Homan, S. R. Jordan, R. Komorowski, A. W. Li, K. McRae, G. Moniz, G. Matsumoto, C. Orihuela, G. Palm, M. Veniant, M. H. Wang, M. Williams, J. D. Zhang, *J. Med. Chem.* **2008**, *51*, 2933 – 2943.
[53] C. Hale, M. Veniant, Z. L. Wang, M. Chen, J. McCormick, R. Cupples, D. Hickman, X. S. Min, A. Sudom, H. D. Xu, G. Matsumoto, C. Fotsch, D. J. Jean, M. H. Wang, *Chem. Biol. Drug Des.* **2008**, *71*, 36 – 44.
[54] H. X. Wang, Z. M. Ruan, J. J. Li, L. M. Simpkins, R. A. Smirk, S. C. Wu, R. D. Hutchins, D. S. Nirschl, K. Van Kirk, C. B. Cooper, J. C. Sutton, Z. P. Ma, R. Golla, R. Seethala, M. E. K. Salyan, A. Nayeem, S. R. Krystek, S. Sheriff, D. M. Camac, P. E. Morin, B. Carpenter, J. A. Robl, R. Zahler, D. A. Gordon, L. G. Hamann, *Bioorg. Med. Chem. Lett.* **2008**, *18*, 3168 – 3172.
[55] D. Q. Sun, Z. L. Wang, Y. M. Di, J. C. Jaen, M. Labelle, J. Ma, S. C. Miao, A. Sudom, L. Tang, C. S. Tomooka, H. Tu, S. Ursu, N. Walker, X. L. Yan, Q. P. Ye, J. P. Powers, *Bioorg. Med. Chem. Lett.* **2008**, *18*, 3513 – 3516.
[56] L. D. Julian, Z. W. Wang, T. Bostick, S. Caille, R. Choi, M. DeGraffenreid, Y. M. Di, X. He, R. W. Hungate, J. C. Jaen, J. S. Liu, M. Monshouwer, D. McMinn, Y. Rew, A. Sudom, D. Q. Sun, H. Tu, S. Ursu, N. Walker, X. L. Yan, Q. P. Ye, J. P. Powers, *J. Med. Chem.* **2008**, *51*, 3953 – 3960.
[57] H. Tu, J. P. Powers, J. S. Liu, S. Ursu, A. Sudom, X. L. Yan, H. D. Xu, D. Meininger, M. DeGraffenreid, X. He, J. C. Jaen, D. Q. Sun, M. Labelle, H. Yamamoto, B. Shan, N. P. C. Walker, Z. L. Wang, *Bioorg. Med. Chem.* **2008**, *16*, 8922 – 8931.
[58] Y. Rew, D. L. McMinn, Z. L. Wang, X. He, R. W. Hungate, J. C. Jaen, A. Sudom, D. Q. Sun, H. Tu, S. Ursu, E. Villemure, N. P. C. Walker, X. L. Yan, Q. P. Ye, J. P. Powers, *Bioorg. Med. Chem. Lett.* **2009**, *19*, 1797 – 1801.
[59] J. Xiang, M. Ipek, V. Suri, M. Tam, Y. Xing, N. Huang, Y. Zhang, J. Tobin, T. S. Mansour, J. McKew, *Bioorg. Med. Chem. Lett.* **2007**, *17*, 4396 – 4405.
[60] N. Vicker, X. Su, F. Pradaux, M. J. Reed, B. V. L. Potter (Sterix Limited, UK), PCT Application: WO2006100502, **2006**, p. 225.

Received: February 25, 2010
Revised: April 12, 2010
Published online on May 18, 2010

